Survey of Photonic Switching Architectures and Technologies in Support of Spatially and Spectrally Flexible Optical Networking [Invited]

Dan M. Marom, Paul D. Colbourne, Antonio D'Errico, Nicolas K. Fontaine, Yuichiro Ikuma, Roberto Proietti, Liangjia Zong, José M. Rivas-Moscoso, and Ioannis Tomkos

***Abstract*—As traffic volumes carried by optical networks continue to grow by tens of percent year over year, we are rapidly approaching the capacity limit of the conventional communication band within a single-mode fiber. New measures such as elastic optical networking, spectral extension to multi-bands, and spatial expansion to additional fiber overlays or new fiber types are all being considered as potential solutions, whether near term or far. In this tutorial paper, we survey the photonic switching hardware solutions in support of evolving optical networking solutions enabling capacity expansion based on the proposed approaches. We also suggest how reconfigurable add/drop multiplexing nodes will evolve under these scenarios and gauge their properties and relative cost scalings. We identify that the switching technologies continue to evolve and offer network operators the required flexibility in routing information channels in both the spectral and spatial domains. New wavelength-selective switch designs can now support greater resolution, increased functionality and packing density, as well as operation with multiple input and output ports. Various switching constraints can be applied, such as routing of complete spatial superchannels, in an effort to reduce the network cost and simplify the routing protocols and managed pathway count. However, such constraints also reduce the transport efficiency when the network is only partially loaded, and may incur fragmentation. System tradeoffs between switching granularity and implementation complexity and cost will have to be carefully considered for future high-capacity SDM–WDM optical networks. In this work, we present the first cost comparisons, to our knowledge, of the different approaches in an effort to quantify such tradeoffs.**

***Index Terms*—Optical fiber communication; Optical networking; Space division multiplexing; Wavelength division multiplexing; Wavelength-selective switches.**

Manuscript received July 22, 2016; revised October 21, 2016; accepted October 22, 2016; published December 15, 2016 (Doc. ID 272038).

D. M. Marom is with the Applied Physics Department, The Hebrew University, Jerusalem 91904, Israel (e-mail: danmarom@mail.huji.ac.il).

P. D. Colbourne is with Lumentum, Ottawa, Canada.

A. D'Errico is with Ericsson Research, Ericsson Telecomunicazioni SpA, Via Moruzzi 1, 56124 Pisa, Italy.

N. K. Fontaine is with Nokia/Bell Laboratories, 791 Holmdel-Keyport Road, Holmdel, New Jersey 07733, USA.

Y. Ikuma is with NTT Device Innovation Center, NTT Corporation, Atsugi, Kanagawa, Japan.

R. Proietti is with the Department of Electrical and Computer Engineering, University of California, Davis, Davis, California 95616, USA.

L. Zong is with the Transmission Technology Research Department, Huawei, Shenzhen, China.

J. M. Rivas-Moscoso and I. Tomkos are with the Athens Information Technology Center, Athens 15125, Greece.

http://dx.doi.org/10.1364/JOCN.9.000001

I. Introduction

The traffic carried by core optical networks as well as the per-channel interface rates required by routers are growing at a remarkable pace, ranging between 30% and 60% year-over-year [1,2]. Fiber-optic transmission and optical networking advancements have so far satisfied these traffic requirements by delivering the burgeoning content in a cost- and energy-efficient manner. However, we are approaching fundamental spectral efficiency limits of single-mode fibers and the growth capabilities of conventional WDM networks operating on a fixed frequency grid are quite limited. While recent advancements and commercial availability of multiple-bit-per-symbol modulation formats, in conjunction with coherent optical reception and polarization division multiplexing, obtain fiber link capacities up to 20 Tb/s, further increases in capacity and spectral efficiency will be very challenging due to nonlinear distortions on account of the optical Kerr effect [3,4]. New optical networking solutions need to be identified to resolve this situation. This paper surveys recent technology innovations in the transport layer driving additional network capacity increases and assesses their projected implementation costs normalized to the capacity gains so as to reveal their potential efficiencies.

The short-term solution to increasing capacity is by introducing hardware enabling elastic optical networking (EON) [5], which is intrinsically related to flexible-grid channel allocation. EON can maximize the spectral efficiency by adapting the provisioned bandwidth to the signal bandwidth, with further efficiencies achievable by assembling subchannels within spectral superchannels [6]. Spectral superchannels, defined as a set of contiguous carriers (subchannels) switched as a single entity from a source to a destination node throughout the network, provide the additional benefit that guard bands between subchannels can be minimized or completely eliminated if spectrally compact multiplexing techniques such as Nyquist

 Journal © 2017 Optical Society of America

WDM or coherent optical (CO) OFDM are employed. However, spectral superchannel transmission imposes requirements on the network-switching elements to support routing spectral slices of varying bandwidths [6]. Enhanced functionality may be offered at the network nodes, such as the capability of all-optically adding/dropping subchannels to/from superchannels, leading to further requirements regarding ultra-fine resolution-filtering technologies [7].

The longer-term solutions will involve extending the fiber capacity beyond the C-band, with two possible routes: increasing the telecom window or introducing parallelism. Multi-band (C-, L-, or S-bands) [8] and multi-fiber (fiber overlays [9]) systems can still rely on elastic optical networking, but space division multiplexing (SDM) systems based on new types of fibers with additional spatial conduits for information transmission offer significant additional opportunities for capacity enhancements [10]. Physical impairments introduced by SDM fibers, such as inter-core crosstalk or mode coupling, and potential benefits of SDM, e.g., cost savings related to the use of common lasers or joint digital signal processing (DSP) [10,11], may make it advisable to route all spatial channels as a single entity across the network. A spatial superchannel is formed by grouping individual spatial subchannels (on different fibers/cores/modes) at the same carrier frequency and leverages on new SDM switching architectures employing switches adapted for operation across the spatial domain [12,13]. A comparison of spectral and spatial superchannel transmission in an SDM–WDM network can be found in [14,15]. Even though spectral allocation strategies result in better network performance, spatial allocation offers the advantage that, by limiting flexibility to a certain extent, cost benefits can be derived from a reduction in the number of required switching elements without compromising the network operation to an unacceptable degree [15,16].

In this paper, we present a comprehensive view of the state of the art of spectrally and spatially flexible reconfigurable optical add/drop multiplexer (ROADM) architectures and their enabling technologies. In Section II, we present a classification of spectral ROADM architectures and discuss the most recent research proposals to achieve cost-effective colorless, directionless, contentionless, and flexible-grid (CDC-Flex) ROADMs. In Section III, we investigate ROADM solutions incorporating sub-band switching capability. SDM switching strategies and associated ROADM architectures are examined in Section IV. An evaluation of the different options to extend the fiber capacity beyond the C-band (multi-band, fiber overlays, and SDM) is discussed in Section V. Finally, in Section VI, we present our conclusions and future outlook.

II. Achieving CDC-Flex ROADM Functionality

Directing wavelength channels throughout optical networks, whether routing at mesh network nodes toward a channel's ultimate destination or simply dropping the channel at an intermediate node and adding another in its place, is performed all-optically by the ROADM switching hardware [17]. The key element of the ROADM node is the wavelength-selective switch (WSS), which performs the tasks of demultiplexing, switching on a wavelength basis, and re-multiplexing in a single compact module. We first describe the function and principal elements of the conventional free-space WSS and then review the historical evolution of the ROADM node in response to its expanding scope in terms of network management of wavelength and direction assignments. We then explore recent research solutions enabling the realization of CDC-Flex ROADMs.

A. WSS Functionality

A standard WSS system configuration is shown in Fig. 1(A), which consists of a linear array of input/output single-mode optical fibers, followed by beam-conditioning optics (fiber-collimating lenses to reduce the beam divergence of the optical fibers, polarization diversity optics for separating each beam into two co-polarized beams, and anamorphic prisms for beam expansion along one direction to illuminate a wide grating section without increasing module height). Following the beam-conditioning optics, parallel collimated elliptical beams are projected onto a diffraction grating. An input beam experiences angular dispersion upon diffraction from the grating, which is mapped to spatial dispersion by a Fourier lens. There are many variants to the basic configuration of Fig. 1(A) in commercial WSSs, such as using a curved mirror in place of the lens or employing a concave grating. These variants may offer greater compactness or reduce component count, but essentially achieve the same function, namely, to spatially disperse and focus the wavelength channels composing the input beam at the lens' back focal plane. Since all beams emerging from the input and output fibers (had light been introduced from the latter) are parallel up to the Fourier lens, following the Fourier lens they all focus to identical positions on a wavelength basis. Thus, at the Fourier lens' back focal plane, the wavelength channels are dispersed and the input/output fiber beams are distinguished by their unique incidence angle. At this plane, where the beams are dispersed and ports spatially superimposed, the switching action takes place by beam-steering the input beam toward a desired output fiber on a wavelength basis [18].

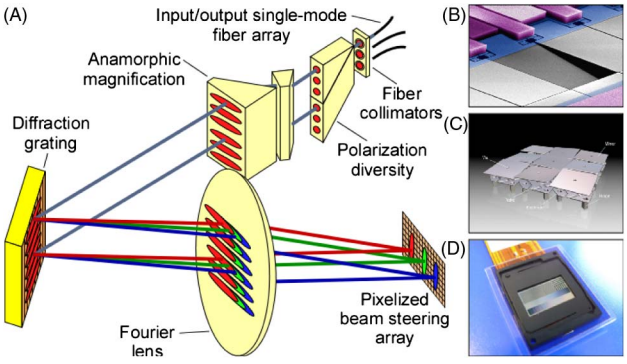

Fig. 1. Elements of a WSS. (A) Optical arrangement for dispersing WDM channels on the beam steering element. Technologies for beam steering include (B) large MEMS tilting micromirrors, (C) fine MEMS tilting micromirrors, and (D) fine LCoS phase modulating pixels. The fine pixels and micromirrors allow flexible WDM channel allocation.

Glossary

A/D	Add/drop
BV	Bandwidth variable
C/L/S-band	Conventional/long/short-band
CapEx	Capital expenditure
CC	Colorless, contentionless
CD	Colorless, directionless
CDC	Colorless, directionless, contentionless
CO-OFDM	Coherent optical OFDM
DGD	Differential group delay
DSP	Digital signal processing
EON	Elastic optical networking
FFT	Fast Fourier transform
FMF	Few-mode fiber
GB	Guard band
HSR	High spectral resolution
LCoS	Liquid crystal on silicon
MCF	Multi-core fiber
MCS	Multicast switch
MEMS	Micro-electro-mechanical system
MIMO	Multiple input, multiple output
NA	Numerical aperture
OFDM	Orthogonal frequency division multiplexing
OpEx	Operational expenditure
OSNR	Optical signal to noise ratio
OTN	Optical transport network
OXC	Optical cross-connect
PL	Photonic lantern
PLC	Planar lightwave circuit
ROADM	Reconfigurable optical add/drop multiplexer
SDM	Space division multiplexing
SLM	Spatial light modulator
SMF	Single-mode fiber
SPOC	Spatial and planar optical circuit
TIDE	Terabit interferometric drop-erase-add
ULI	Ultrafast laser inscription
WDM	Wavelength division multiplexing
WGR	Waveguide grating router
WSS	Wavelength-selective switch
WSXC	Wavelength-selective cross-connect

Early WSSs utilized micro-electro-mechanical system (MEMS) tilting micromirrors for beam steering, one micromirror per wavelength channel. Switching was performed by redirecting the incident input beam on a wavelength channel basis by individually tilting each micromirror, so as to reflect from the micromirror in a direction commensurate with the desired output fiber [19]. Upon reflection, the beam back-traces the optical elements and then efficiently couples to the selected output fiber. The width of the channelized MEMS micromirrors [see Fig. 1(B)] must match the WDM channel plan of the optical network over which it is to be deployed (e.g., 50 or 100 GHz), and the optical spectrum must be well aligned to the device. The advantage of the MEMS micromirror approach is their optical performance, as the mirror reflectivity is high, uniform, non-scattering, and independent of switching angle. A flexible-grid mode of operation can be achieved by employing MEMS tilting micromirrors on a finer pitch and tilting them in groups, so that the channel center wavelength and bandwidth can be adaptively defined and made to match the signal bandwidth [20]. In place of customized MEMS micromirror arrays, ones modified from the image-projection industry can be substituted, with switching obtained by setting all the small, two-dimensional micromirror pixels falling under the wavelength channel of interest to switch to the desired port [21] [see Fig. 1(C)]. Alternatively, another technology adapted from the display industry may be employed, based on a two-dimensional liquid-crystal on silicon (LCoS) spatial light modulator (SLM) [22] [see Fig. 1(D)]. Here, the liquid-crystal layer needs to be modified from amplitude to phase modulation, and switching is performed by writing a linear phase ramp (the equivalent to a mirror tilt). Since the phase-modulation depth that can be inscribed by the LCoS SLM is limited to 2π, the phase ramp is applied modulo 2π and forms a blazed grating. As such, its optical performance degrades with increasing steering/diffraction angle, giving rise to reduced efficiency (or port-dependent loss) and spurious diffraction orders creating crosstalk to neighboring ports [23]. The main advantages of using two-dimensional SLM technologies adapted from the image-projection industry are the wide availability of devices (circumventing custom MEMS development efforts), the intrinsic support for flexible channel definition by software programming, and fine spectral channel boundary control (at the sub-pixel level) by preferentially allocating edge pixels to the two boundary channels [24]. This allows a WSS to be adapted from a coarse to a fine WDM grid, or to operate in a flexible-grid fashion in support of elastic optical networking [25].

Finally, note that since all input and output fiber port beams are imaged in the wavelength-dispersed plane to common positions, switching cannot be performed for more than one input beam to two different independent outputs. Hence, the operation of the WSS is restricted to a single input, multiple output case, denoted $1 \times K$ WSS, allowing the input wavelengths to be distributed to the K output fibers; alternatively, the WSS can operate with multiple (K) inputs and a single output, denoted $K \times 1$ WSS, in which the connection from the desired input to the output fiber is established independently for each wavelength channel.

B. ROADM Node Evolution

ROADM node architecture has evolved in lockstep with WSS technology over the past 15 years, as the two are intimately entwined. In Fig. 2, we chart the expanding capabilities of the ROADM node and its evolution toward CDC-Flex functionality.

1) Blocker-Based Add/Drop Node: Early ROADM nodes were placed in bi-directional optical transmission systems (long-haul line systems or metro-scale rings, where intermediate add/drop access to optical channels was required). These implementations were based on "wavelength blockers," as shown in Fig. 2(i), which are merely 1×1 WSS (single input, single output) [26–28]. Their role is to clear the bandwidth occupied by the "drop" channel so that an

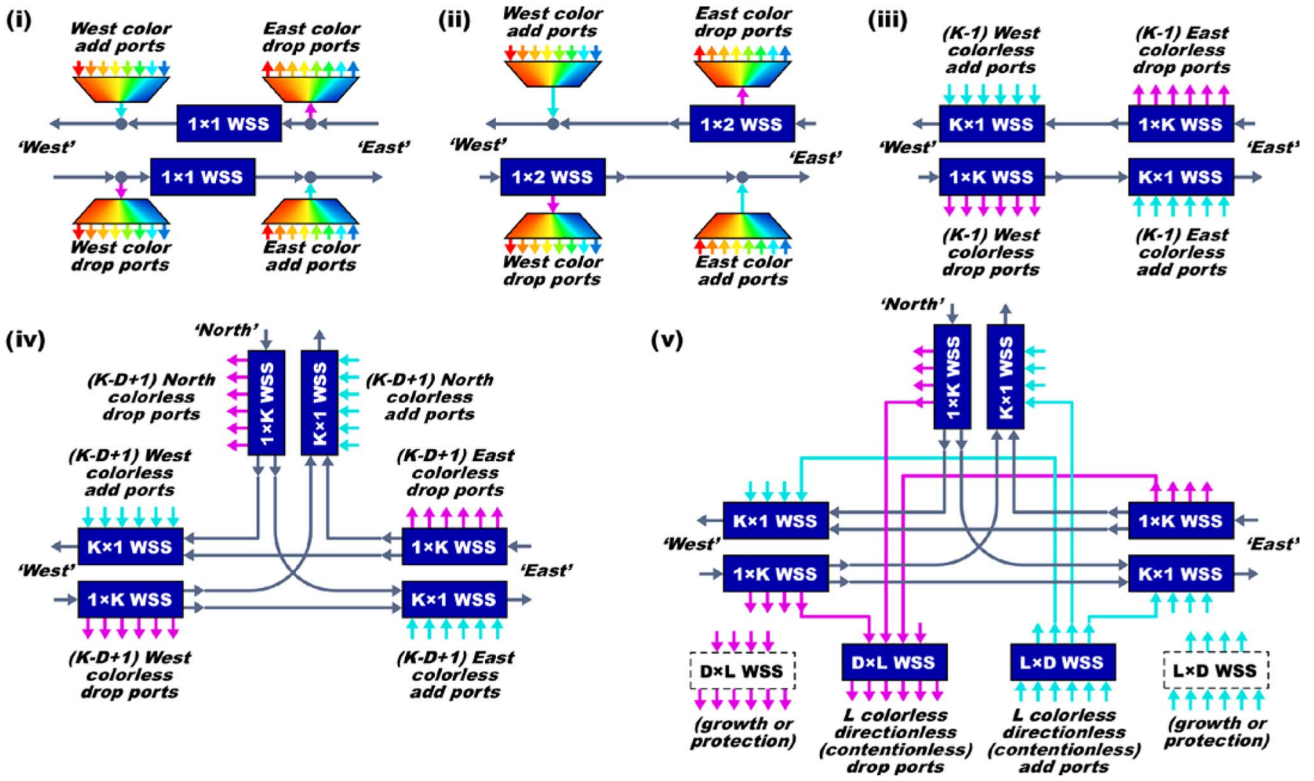

Fig. 2. Evolution of the network ROADM node architecture. (i) Blocker (1 × 1 WSS) based add-drop node and (ii) 1 × 2 WSS based add-drop node for line systems with colored add/drop ports, (iii) colorless ROADM with $1 \times K$ WSS, with $K - 1$ add/drop ports, (iv) degree three-mesh network node with cross-connect functionality and colorless and contentionless (but direction-bound) add/drop, and (v) mesh network node with colorless, directionless, and potentially contentionless (depending on $D \times L$ WSS capability) add/drop. The WSS can provide flexible-grid attribute, depending on the employed switching technology.

"add" channel can be inserted in its place without suffering from deleterious crosstalk from the remnants of the "drop" signal.

2) 1×2 *WSS-Based Add/Drop Node:* Expanding the WSS to 1×2 functionality allows for better loss management within the ROADM node, as it eliminates a passive splitter [Fig. 2(ii)]. In both the 1×1 and 1×2 WSS cases, the "drop" channels appearing on the drop fiber are then demultiplexed (and "add" channels multiplexed) onto individual transceivers, each associated with a unique wavelength ("color" port). Since tunable wavelength lasers could be had only for a significant premium at the time, optical transceivers were associated with a particular fixed wavelength, and having color ports was not considered a serious impediment. However, this implied that, for unrestricted flexibility in choosing the "drop" wavelength channel during network operation, transceivers at all wavelengths had to be deployed at each ROADM node, which was clearly not an economically viable solution. Hence, a smaller number of add/drop transceivers at preselected wavelengths were deployed, thus limiting the operational flexibility in routing channels to the desired ROADM node, which further constrains network management.

3) $1 \times K$ *WSS-Based Colorless Add/Drop Node:* In support of greater operational flexibility, and with the advent of wavelength-tunable transceivers, the WSS output port count grew to a $1 \times K$ design [with $K = 9$ being a popular choice, as for a 40-channel WDM system it allowed 8-channel (20%) wavelength access]. This allowed for "colorless" add/drop ports following the solution of Fig. 2(iii). Having colorless ports allows for efficient wavelength routing within the optical communication system; as long as a drop port is available and is terminated by a transceiver, any wavelength can be directed to it (i.e., the ROADM is "contentionless," as the WSS hardware imposes no wavelength contention).

4) $1 \times K$ *WSS Colorless/Contentionless Mesh ROADM Nodes:* Adding WSS support of switching to multiple outputs allowed all-optical networking to come to fruition. Optical networks typically follow a mesh architecture, having nodes with varying numbers of links to neighboring nodes. The degree of the node denotes how many fiber links to neighboring nodes are attached to it (e.g., degree 3, 4, etc.). Wavelengths can be routed from any ingress of the network node to any egress fiber, or channels can be locally dropped, following the "Route-and-Select" arrangement of Fig. 2(iv) [29]. This introduces cross-connection capability at the ROADM node between the fiber links in addition to add/drop support. Here, a $1 \times K$ WSS at each ingress fiber port distributes the incoming wavelength channels toward egress fiber ports or to colorless drop ports. At the egress fiber ports, a $K \times 1$ WSS combines the routed and added

channels to the output WDM fiber. (There exists a "Broadcast-and-Select" alternative arrangement that replaces the ingress $1 \times K$ WSS with passive splitters, as a lower-cost option [30].) The add/drop ports that are directly attached to the WSS at the ingress and egress fibers are associated with that direction. This can be considered as a limitation, as demonstrated next: Suppose each ingress fiber has a finite number of drop transceivers deployed, and one direction's drop count is fully occupied. If another wavelength channel is to be dropped from that fully occupied direction, the request cannot be fulfilled even though there are available idle transceivers at the node's other ingress ports. Yet the wavelength channel cannot reach this resource, as it is bound to a direction. Hence, this architecture inherits the colorless and contentionless attributes but the add/drop ports are direction-bound.

5) Colorless/Directionless/Contentionless ROADM Nodes: To derive maximum benefit from node transceivers, it is desired that they be "directionless," and hence able to serve drop (add) channels arriving from (directed to) any network link connected to the node. This can be achieved by adding additional hardware that serves to aggregate the directions and distribute the add/drop channels to the available transceivers. One possibility is to introduce optical cross-connect (OXC) functionality using a fiber space switch (non-wavelength-selective) to the WSS-based ROADM node. The OXC may be placed within the WSS interconnectivity [31], or only at the drop ports of all directions, and establish connections to the transceivers [32]. Another possibility is to use a WSS operated with multiple (D) input fiber ports, matching the direction count, and multiple (L) output fiber ports for transceiver access (i.e., $D \times L$ WSS), Fig. 2(v). However, as noted earlier, all input and output fiber ports are imaged to the same position within a WSS, which implies that it cannot handle multiple inputs and outputs simultaneously for independent switching. Hence, the caveat in this implementation of a $D \times L$ WSS is that any particular optical wavelength can only appear on one input port at most. Thus, the node architecture is restricted to drop only a single occurrence of a particular wavelength among all the node's ingress links, which represents contention for the drop wavelength choice in network routing. Therefore, due to the inherent limitation of the conventional WSS, this node is classified as a colorless, directionless (CD) ROADM, which falls short of providing full CDC-ROADM functionality that system operators desire.

A CDC-ROADM solution is possible, based on a multicast switch (MCS) solution for the add and drop wavelength channels. An MCS splits the drop signals and delivers a copy of all the drop channels to each attached transceiver. A multiple-input, single-output fiber switch (non-wavelength-selective) determines which direction will be attached to the transceiver. A tunable wavelength filter may be required to isolate a single drop channel from the selected direction. However, for coherent detectors, this filter may be discarded. The tunable filter at the drop ports may limit the channel bandwidth, hence impacting the support for channel flexibility and elastic optical networking. Since most elastic networking solutions utilize coherent detection, this should not be a detriment. While the MCS-based solution provides the full CDC functionality using rudimentary elements of splitters and selector switches, it is hampered by the high splitting losses inherent to the MCS solution. Therefore, an MCS architecture must be accompanied by an optical amplifier array to compensate for these losses, which adds to the cost of this solution, increases the power consumption due to the optical amplifiers, and degrades the signal's OSNR. These shortcomings have hampered the widespread acceptance of the MCS-based CDC-ROADM.

ROADMs which employ passive demultiplexers in their implementation (i.e., blocker and 1×2 WSS solutions) are bound to the channel allocation plan of the demultiplexer. ROADM architectures based solely on WSS inherit the channel flexibility from the WSS attributes. Hence, if a flex-grid WSS performs all the channel routing, then the ROADM node can support elastic optical networking [33]. CDC-Flex-ROADM capabilities generate considerable interest in the optical communication industry, in support of contentionless connection of any wavelength (and with any bandwidth and modulation format) from any transceiver in any direction. This guarantees that the node can evolve with the modulation formats being deployed and support elastic optical networking with bandwidth-variable transceivers, making the solution future-proof. CDC-Flex-ROADMs are further advantaged by imparting the network with higher programmability, simplified management (less-restrictive routing constraints), and greater survivability of transceiver failure. However, the additional hardware required for their implementation leads to increased node cost (i.e., CapEx increase), as well as possible extra complexity of intra-node fiber connections, node volume, and sensitivity to failure of the direction aggregation hardware (possibly impacting all node channel drops or adds unless protection means are introduced with additional implementation complexity). Moreover, the MCS-enabled CDC-Flex-ROADM requires additional amplifiers impacting cost and power dissipation (additional OpEx), while the $D \times L$ WSS enabled Flex-ROADM offers only CD flexibility, which constrains operations. Hence, the lack of an effective CDC-Flex-ROADM solution that simultaneously achieves all desired attributes has hampered its deployment by network operators, who are still seeking technological advances in switching hardware to enable better CDC-Flex-ROADM solutions.

C. Beyond the State of the Art on CDC-Flex-ROADM

In order to address CDC-Flex-ROADM requirements without significantly increasing cost, footprint, and complexity, technological upgrades of current devices will play a crucial role. New requirements need to be addressed in future high-capacity flexible-grid optical nodes. Next-generation optical nodes will incorporate higher levels of flexibility in switching, bandwidth, and transmission rate. The introduced flexibility will allow dynamic composition of network functions to cope with heterogeneous traffic demands. The CDC-Flex operation in the ROADM nodes gives the possibility of optimizing the resource utilization,

to reconfigure the network according to the variation of the traffic pattern in a cost-effective way, while also supporting re-routing functions in case of faults.

1) Ultrahigh-Port-Count WSS: Realization of ultrahigh-port-count WSS can lead to an alternative CDC-Flex-ROADM solution. High port counts may be challenging to realize using a WSS design based on discrete elements. An optical system that uses a guided-wave solution in combination with free-space optics, termed *spatial and planar optical circuit* (SPOC), has been demonstrated (see Fig. 3). A SPOC-based WSS replaces some of the elements of the front-end beam-conditioning optics with a waveguide-based solution that serves as a spatial beam transformer. It applies a waveguide grating router (WGR) of zero diffraction order (non-dispersive) to each fiber port, thereby anamorphically broadening each output radiating beam (Fig. 3, top), obviating the need for a microlens array and anamorphic prisms and alignment procedures. The launched parallel beams are collimated in the fast axis by a single cylindrical lens, followed by the standard elements of the WSS (polarization and dispersive optics, and an LCoS SLM) (Fig. 3, bottom). A SPOC-based WSS was used to demonstrate a record 1×95 WSS configuration [34]. Similarly, an adiabatic waveguide broadening section may be implemented instead of the zero-order WGR, as shown for a 1×40 WSS [35] and for a 1×93 WSS [36]. Both the zero-order WGR and the adiabatically broadened waveguide essentially perform the same task of converting each individual I/O beam into a broad mode profile along the guided direction, hence eliminating the need for placing a microlens array and achieving very high beam fill factors (defined as beam size/port pitch) for high port packing.

With ultrahigh-port-count WSS elements, the CDC-Flex-ROADM can aggregate individual drop ports from each direction to a selector switch (non-wavelength dependent) placed in front of each deployed transceiver (Fig. 4).

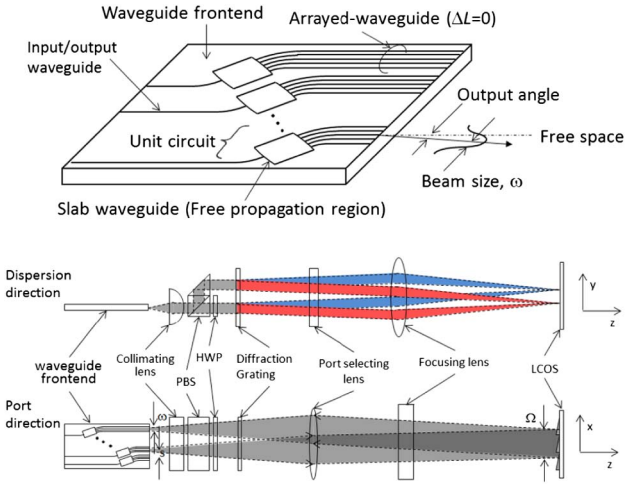

Fig. 3. High-port-count WSS utilizing a PLC front end for high-density packing of fibers and implementing part of the anamorphic optics solution. *Top*: SPOC design. *Bottom*: Optical arrangement of the high-port-count WSS with LCoS switching technology for wavelength flexibility.

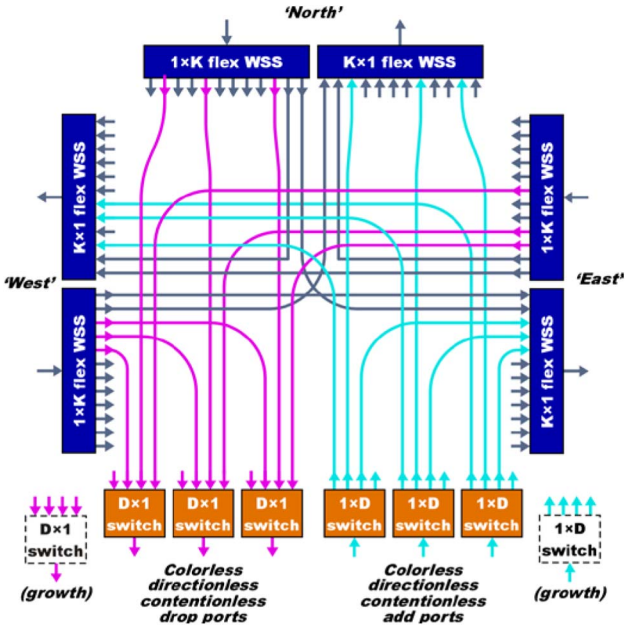

Fig. 4. CDC-Flex-ROADM implementation with high-port-count WSS. Each add/drop port incorporates a direction-selection switch.

The number of add/drop transceivers supported by the node is nearly equal to the WSS port count ($D-1$ WSS ports are required for through-node traffic routing; the rest for add/drop port support). This architecture is advantaged by having very low loss budget to reach the transceiver, as well as having a per-transceiver aggregation means, thus circumventing the common aggregator that can lead to an ungracious failure mode. On the down side, there is an inherent inefficiency to this solution where on average only $1/D$ of the drop ports of any direction WSS are utilized [as $(D-1)/D$ are allocated to drop ports from other directions]. This means that while the high-port-count WSS will command a cost premium, most of these extra ports will be unutilized (considered the cost of implementing CDC functionality). As these WSSs use LCoS SLMs, the solution is an inherently flexible grid.

2) Multi-Input, Multi-Output WSS for Port Aggregation: Another WSS alternative that is instrumental for achieving the full CDC-Flex-ROADM requirements is a contentionless $D \times L$ WSS (having D input ports and L output ports and used for add/drop port aggregation). A contentionless $D \times L$ WSS can support multiple input ports with the same wavelength channel appearing across more than one of its input ports. As explained earlier (Subsection II.A), all input and output fiber beams are imaged in the wavelength-dispersed plane to a common position. This degeneracy has to be broken, which can be achieved by having a unique position for the dispersed spectrum for each of the D input (direction) ports, and introducing the means to route each output (drop) port to a selected dispersed spectrum.

One way of achieving a contentionless $D \times L$ WSS is to use a modified SPOC device, designed not only to broaden

a beam but also to prescribe a spatial tilt across it. This is achieved by exciting the zero-order WGR with an off-center mode (see Fig. 5, top). An offset excitation of the waveguide array generates a linearly varying spatial phase, which is preserved at the PLC facet. Here, D input waveguides excite a single, central WGR of the SPOC through a slab lens at distinct positions, thereby serving to collimate all inputs simultaneously while further instilling a unique tilt angle to each one due to the Fourier transform property of the confocal slab lens. The subsequent free-space optical arrangement maps each tilt to a unique, offset position on the LCoS SLM (see Fig. 5, bottom). A wavelength channel can then be routed from any of the D input dispersed signals to a desired output port (of the L available), by beam-steering toward the port position on the SPOC device. There, the beam couples to the WGR associated with the desired output destination. Since the incidence angle onto the output-side WGR depends on the input port source, the signal will emerge at one of the D waveguides attached to the destination slab lens (the actual waveguide depends on the source input fiber). Hence, an active $D \times 1$ switch is placed afterward to select which of the D waveguides is connected to the output fiber. This contentionless $D \times L$ WSS is also an inherently flexible grid due to the LCoS switching engine, and can be placed within the architecture of Fig. 2(v), enabling CDC-Flex-ROADM functionality. A SPOC-based contentionless 8×24 WSS was demonstrated in [37].

The contentionless $D \times L$ WSS can also be implemented without resorting to a SPOC element for the beam conditioning optics. As the beam-delivery optics (from the input fibers and dispersive optics that generate the separated dispersed spectra on the LCoS SLM) slightly differ from the beam-reception optics (from the LCoS SLM to the output fibers including an active switching element), they require unique arrangements that are placed side by side [38]. Its scaling potential was studied in [39], where 8×128 WSS functionality was designed and simulated. However, having unique optical arrangements for the input and output beam delivery optics leads to a cumbersome arrangement.

An alternative, simplified free-space arrangement was recently demonstrated [40], where MEMS tilting micromirrors were placed on every fiber port for beam-steering to the unique positions on an LCoS SLM (where the fiber spectra are dispersed), as shown in Fig. 6. This arrangement also allows for contentionless $D \times L$ WSS functionality, with the added benefits that the optical system is fully symmetric (same optical elements in the path from fiber to spectral plane and back, simplifying the optical design) and the number of input fiber ports, D, can be software-reconfigured according to the ROADM degree size, with the remaining fiber ports thereby available to support additional drop ports. For example, contentionless 8×24 WSS functionality is possible for degree 8 nodes (which occur with reduced frequency). Should the node be of degree 4, the WSS can be reprogrammed as 4×28, making optimal use of the fiber port resource and availing extra drop ports.

Contentionless $D \times L$ WSS serves to distribute dropped channels to transceivers from any direction and likewise aggregate added channels to egress fibers for CDC-Flex-ROADM realization. Due to the lower losses of this solution compared to the inherent losses of an MCS, the use of optical amplifiers can be avoided. Note that optical amplifiers can also be dropped in the MCS case if the node is constrained to support a very small number of transceivers. While $D \times L$ WSS tries to maximize the drop port count, L, it is possible to have a low-port-count MCS, e.g., 6×6, which reduces the inherent losses by decreasing the split ratio. However, this solution reduces the scalability of the network node. Fiber connectivity is also greatly reduced for a $D \times L$ WSS implementation, as dropped channels from each direction are still WDM multiplexed and only separated at the $D \times L$ WSS [compare fiber count in Figs. 2(v) and 4].

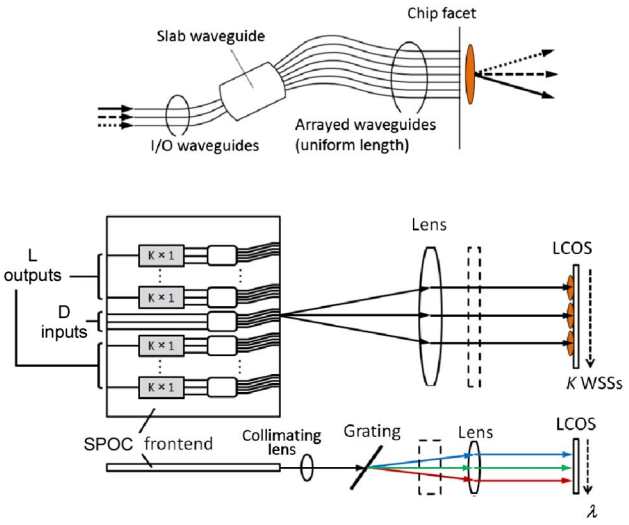

Fig. 5. Contentionless $D \times L$ WSS utilizing a PLC front end. *Top*: SPOC design variation. *Bottom*: Optical arrangement of the contentionless $D \times L$ WSS with LCoS switching technology for wavelength flexibility.

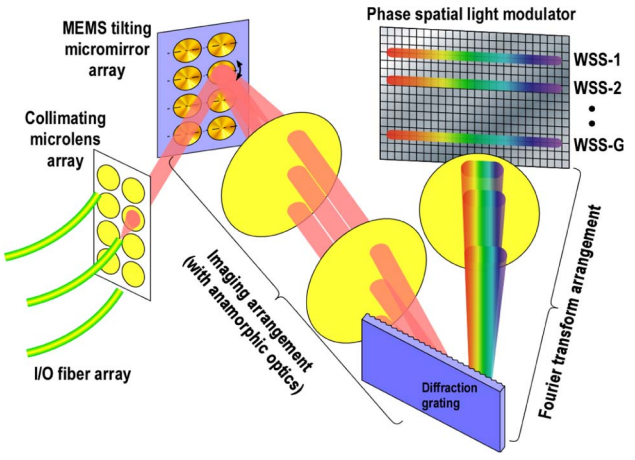

Fig. 6. Port-reconfigurable WSS array setup using free-space optics. MEMS micromirrors at the fiber beam path enable assignments of the input/output ports for different realization of contentionless $D \times L$ WSS, matching the node size.

3) Wavelength-Selective Cross-Connect: A final variation for CDC-Flex-ROADM implementation utilizes a wavelength-selective cross-connect (WSXC). A WSXC was first demonstrated by combining optical multiplexers/demultiplexers with an optical cross-connect (fiber switch fabric) [41]. However, the use of fixed demultiplexers subjects the switch to a channel grid. By switching dispersed light with an LCoS SLM, the WSXC obtains channel flexibility. Since cross-connect functionality requires two beam-steering events to complete arbitrary connections from any input to any output, the optical system is complicated by the fact that it must perform an imaging operation between the two beam-steering planes, as first demonstrated in [42] for a 5×5 WSXC, or the spectral resolution of the channel definition would worsen (as implemented in [43]). A new, greatly simplified realization of an 8×8 WSXC was demonstrated recently [44] (see Fig. 7). Beam conditioning optics (collimators, cylindrical lenses, anamorphic prisms, polarization diversity, and a diffraction grating) applied to the input fibers disperses the 8 inputs onto the first LCoS SLM. On the output side, an identical arrangement disperses light from the output fibers to the second LCoS SLM (the light is actually traversing the elements in reverse). A special relay-imaging system between the first and second LCoS SLMs images the dispersed light in the wavelength-dispersed direction and Fourier-transforms it in the port direction (required for switching with beam-steering technology). Such an 8×8 WSXC can perform any permutation on a wavelength basis between the input and output set without contention and with flexible channel definition due to the use of LCoS technology.

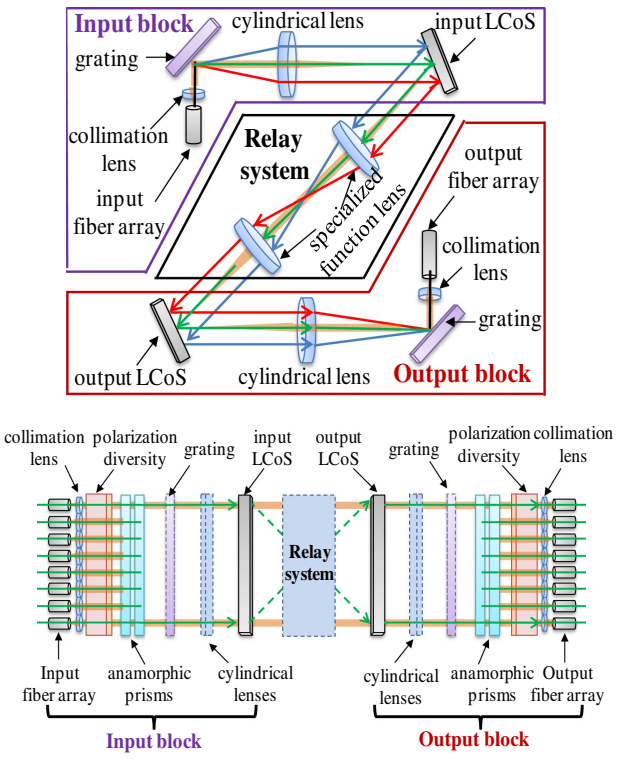

Fig. 7. Schematic of the optical prototype of the 8×8 flex WSXC. *Top*: Free-space propagation in the dispersion direction. *Bottom*: Details of free-space propagation in the port direction.

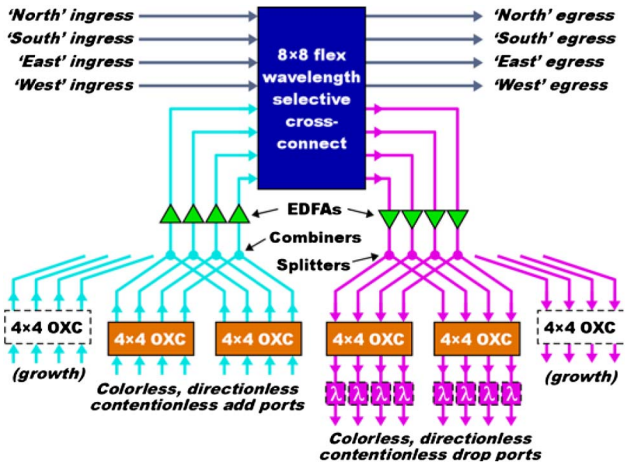

Fig. 8. Possible architecture of CDC-flex ROADM based on WSXC. Drop ports require tunable filters, which may be omitted for coherent receivers.

A suggestion for how to deploy such an 8×8 WSXC for a CDC-Flex-ROADM functionality in a degree-4 node is shown in Fig. 8 [45]. Four of the inputs and outputs handle the ingress and egress node fibers. The remaining four inputs and outputs carry the traffic to be dropped and added. Multiple replicas of the four drop fibers are created, necessitating ancillary optical amplification (similarly on the add side, where input sets are passively combined). Each copy set of four fibers feeds a small space switch of dimension 4×4 for routing drop channels to an available transceiver. The multiple copies made by passive splitters are required to increase the number of supported add/drop transceivers. Any dropped/added wavelength channel from any direction can reach an available transceiver by selection of an available wavelength slot on the WSXC and configuration of the small OXC. Since the dropped channels are wavelength multiplexed, a tunable filter may be required in front of the transceiver if direct detection is employed. Note that an alternative 8×8 Flex-WSXC functionality was also recently demonstrated utilizing a SPOC front-end design for spatial beam transformation [46]. The salient features of a CDC-Flex-ROADM based on a single WSXC are the small number of components required for its implementation and simple fiber connections within the node, as the various cross-connections are carried out in free-space within the switch confines. However, should the single WSXC fail, all traffic through the node is interrupted. Additional architecture variants for use of a WSXC in a CDC-Flex ROADM, including $1 + 1$ protection coverage, are introduced in [47]. The cost benefits and architectural simplicity of this solution when protection is introduced are then reduced.

III. Spectrally Flexible Sub-Band ROADM

Flex-grid ROADM solutions allow for adapting the network-provisioned bandwidth to the wavelength channel's spectral support—the basis for EON. However, due to the WSS spectral transfer function [19], which provides a "clear channel bandwidth" narrower than the

provisioned bandwidth, the provisioned bandwidth must always be larger than the channel bandwidth if the channel is to be routed in the network independently. The determining factors in this over-provisioning are the WSS spectral roll-off bandwidth from the "pass" to "block" state, which is directly related to the WSS spectral resolution, as well as the number of ROADM nodes the signal will traverse, as each passage through a WSS represents another channel-filtering event. Hence, when elastic optical channels are assigned to the network, they must include spectral guard bands (GBs) between adjacent channels to allow for independent network routing. A GB is also required to take into account center wavelength accuracy, component aging, temperature dependence, manufacturing tolerances, etc. These GB form an inherent inefficiency, as their spectral support cannot be utilized for carrying information. One way of increasing the spectral utilization is to combine several carriers into one superchannel to be routed as a single entity, thus obviating the need for inter-subchannel GBs. Consider the emerging transmission of 400 Gb/s superchannels, which are typically composed of two closely spaced 200 Gb/s Nyquist-shaped carriers (at 16 QAM over dual polarizations) [48], which can be contained within 75 GHz of provisioned bandwidth. In this case, channel filtering is negligible even if the 400 Gb/s signal traverses multiple ROADM nodes (see Fig. 9). Detection of this dual-carrier superchannel format is accomplished with a power splitter followed by two coherent detectors.

However, there are scenarios where we wish to enjoy the benefits of superchannel routing throughout the optical network (minimizing GB and thus maximizing spectral utilization) as well as provide sub-carrier add/drop capability within the superchannel at certain network nodes for operational flexibility. This can be done by deploying a full OTN superchannel transceiver for adding and dropping subchannel tributaries electronically and creating a new superchannel in its place [49]. An alternative hybrid optical/electronic-based solution, SERANO [33], utilizes optical splitters for broadcasting a dropped superchannel to multiple fixed subchannel receivers directly coupled to tunable transmitters, only part of which are turned on to create new superchannels composed of regenerated subchannels that can also be wavelength converted, thus further dealing with defragmentation. However, the cost basis of these solutions, requiring at minimum banks of subchannel coherent receivers and transmitters when only a single channel add/drop might be required, is exorbitant. Instead, the research community is seeking specialized ROADM solutions which can perform the add/drop functionality all-optically [7]. Such all-optical subchannel grooming capability has been proven to be able to improve network performance [50] and reduce the total equipment cost as compared to optical networks based on end-to-end superchannel transmission [51] and multi-layer networks with built-in electronic aggregation [52]. The solutions for supporting sub-band ROADM differ depending on whether the subchannels composing the superchannel are spectrally overlapping or not.

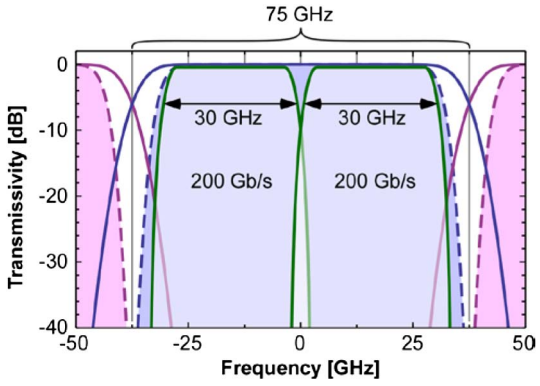

Fig. 9. Dual-carrier 400 Gb/s superchannel with spectral support within single WSS transfer function provisioning 75 GHz WSS bandwidth (solid blue line) and a cascade of 10 WSSs (dashed blue line). Each Nyquist-shaped carrier is modeled as a 30 GHz wide (25 GHz + 20% overhead) raised cosine channel with 0.2 roll-off factor. Channels' carriers are separated by 31.25 GHz.

A. Subchannel Optical Add/Drop of Spectrally Non-Overlapping Signals

With digital signal pre-processing, an optical transmitter can create modulation formats that are spectrally efficient, having nearly rectangular power spectrum (e.g., Nyquist-WDM and CO-OFDM). Such transmitters can be used to create the multiple subchannels comprising the superchannel. The subchannels can be set contiguously to create a continuous superchannel, when no intermediate add/drop support is required. However, when optical subchannel extraction from the superchannel is required then minimal GB should be placed on either side of the subchannels to be dropped, along with fine filtering technology to assist in selecting the subchannel. The size of the GB is commensurate with the fine filter's optical resolution.

An optical filter specially designed to filter arbitrary subchannels from a superchannel was first reported in [53]. The high spectral resolution (HSR) filter employed a waveguide grating router as the dispersive element instead of a bulk diffraction grating, for customizing the resolution and operational bandwidth. The WGR was designed with a free spectral range of 200 GHz (i.e., operating bandwidth), and its number of waveguide arms (250) was selected to achieve 1 GHz optical resolution. A superchannel introduced into this WGR-based processor is angularly dispersed and its frequency components spatially dispersed at a Fourier lens back focal plane (Fig. 10), where a spatial light modulator acts to pass or block arbitrary spectral components at fine resolution for adaptive filtering of subchannels. The filtering arrangement is very similar to that of a WSS (Fig. 1), where the main difference is the spectral support (200 GHz versus C-band) and optical resolution (1 versus ~7.5 GHz), both of which are determined by the dispersive element. In order for the WGR to well resolve such fine spectral features, its waveguide delays have to be very large, which represents a challenge for maintaining the optical phases at the WGR output facet due to fabrication tolerances. Two

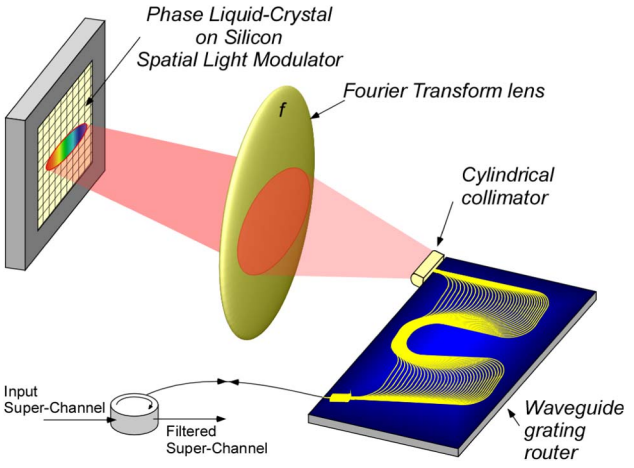

Fig. 10. Fine-resolution spectral filter (single input, single output), utilizing a specially engineered WGR to span a typical superchannel bandwidth of 200 GHz and resolve fine spectral features of 1 GHz within. Spectral blocking regions are selected at 400 MHz addressability with an SLM in the Fourier plane.

techniques have been developed for correcting the WGR phases post-fabrication, one based on a secondary phase SLM in an imaging configuration [53], and the other on waveguide phase trimming with UV laser irradiation [54].

Such a fine-resolution filter can be employed within a CDC-flex ROADM architecture following a dual-level hierarchical approach, with the top level performing superchannel network routing using route-and-select topology and the lower level handling subchannel access (Fig. 11). At the top network routing hierarchy, a CDC-flex ROADM aided by direction-side WSS performs superchannel routing from ingress to egress ports, or superchannels

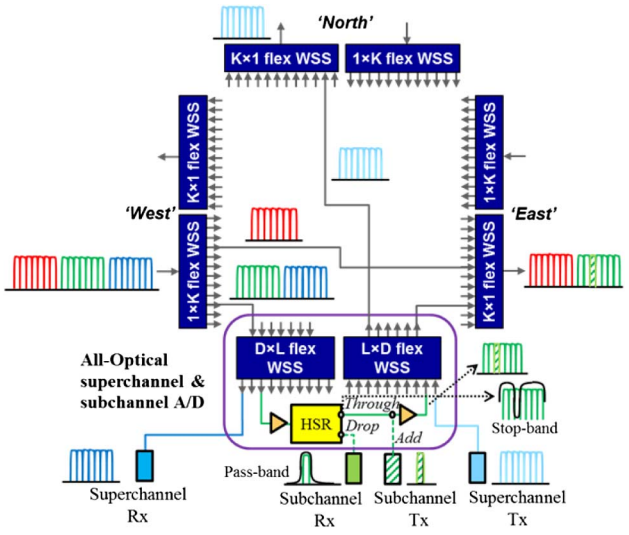

Fig. 11. CDC-flex-ROADM extended to support subchannel add/drop from network level superchannels. A selected superchannel is split, with one copy incident on a subchannel coherent receiver and the other copy fine filtered to clear the bandwidth for an added subchannel.

selected for drop are directed toward a $D \times L$ WSS. A complete superchannel can be dropped and detected by a full coherent receiver, and another superchannel can be introduced to the network in its place. Alternatively, at the lower superchannel hierarchy level, we can access subchannels following a blocker-based ROADM architecture [Fig. 2(i)]. The superchannel is split, with one copy destined to a single (or multiple) subchannel coherent detector and the second copy being filtered at fine resolution by the HSR filter, which clears (or blocks) the bandwidth corresponding to the single or multiple subchannels that have been dropped. New "add" subchannels are introduced into the available spectral slots via an optical coupler, reconstituting the superchannel as a contiguous entity for reinjecting back to the optical transport network. Consider the networking functionality for three superchannels (red, green, and blue), each composed of seven subchannels introduced to the ROADM node from the West direction. The red superchannel is routed as a whole to the East direction. The blue superchannel drops locally its entire contents and a new superchannel is added (cyan) and sent out the North direction. The green superchannel is also dropped but then further processed to drop a single subchannel and introduce a new one (green striped) in its place after filtering with the HSR filter.

Having the capability to filter subchannels at 1 GHz optical resolution allows for their extraction with only 2 GHz wide GB set between subchannels. As the filter further supports spectral addressability of 400 MHz (the mapping of an SLM pixel size to frequency offset), the subchannels' bandwidth can be defined with full flexibility. However, for operational ease, it is simpler to define a finite spectral slot size by which spectrum is reserved, in this case 3.125 GHz following the ITU trend of halving the grid size [55], which leads to nearly optimal spectral occupancy according to [56]. Figure 12 demonstrates a 200 GHz wide superchannel (spanning 64 spectral slots), provisioned over 218.75 GHz (70 spectral slots), that incorporates 9 subchannels of varying widths

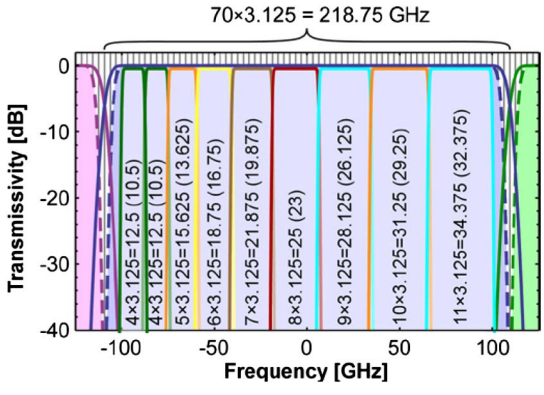

Fig. 12. Exemplary superchannel packing with subchannels of varying bandwidth, when the HSR filter has 1 GHz resolution. Subchannel spectral granularity of 3.125 GHz used (example shows 4, 5, …, 10, 11 slot assignments, total of 64 slots = 200 GHz assigned), with the net subchannel bandwidth in parentheses, with 2 GHz reserved for an inter-subchannel GB. WSS superchannel boundary in solid blue line, and cascade of ten WSSs in dashed blue line.

(4 to 11 slot assignments, demonstrating complete flexibility in subchannel bandwidth assignment according to the EON concept), with each subchannel having a clear bandwidth 2 GHz smaller than the spectral assignment since a GB is assumed about each subchannel (a worst-case scenario which implies each subchannel will be dropped somewhere along the superchannel path). Even with nine subchannels and their inter-subchannel GBs, the superchannel provides 182 GHz of clear bandwidth for data payload at any modulation format. The unutilized bandwidth ($218.75 - 182 \cong 37$ GHz, or 17%) is roughly equally divided between inter-subchannel GBs and superchannel edges (three spectral slots on each side) required for supporting network routing (fiber networking level GB). In [57], simulation results of Nyquist-WDM transmission through a cascade of ROADMs with ultra-selective A/D modules were presented, showing that the edge subchannels are more affected by the two filtering stages, as was confirmed in experiments [58]. A loop experiment demonstrating the ability to repeatedly drop and add the same subchannel from within a superchannel was recently demonstrated [59].

An alternative approach for optical filtering non-overlapping subchannels from a superchannel can be based on a fixed, high-resolution, low free spectral range demultiplexer. High-resolution demultiplexers can be obtained by combining finite and infinite impulse response devices (i.e., chip scale interferometers assisted by high Q-factor microring resonators). The use of a fixed device for separating a superchannel to its constituent subchannels implies that the subchannels must reside on a fixed, predetermined grid, thereby losing the flexibility trend of EON. In addition, each subchannel experiences filtering operations, regardless of whether the subchannel is required to be isolated for add/drop operation. To its advantage, the filtering device can be fully passive, though in practice the high-Q microrings need active thermal stabilization to keep their resonance wavelength locked. A ring-assisted, sharp 12.5/25 GHz interleaver was designed for separating 12.5 GHz wide subchannels from a superchannel [60], and its cascadability in loop experiments was studied [61].

B. Subchannel Optical Add/Drop of Spectrally Overlapping Signals

Supporting add/drop operations with GBs between subchannels enables simple extraction with optical filters, but the inserted GBs reduce the spectral utilization. Moreover, a superchannel can be constructed with overlapping carriers, as is the case in a CO-OFDM signal spanning the entire superchannel. Under these circumstances, a different subchannel add/drop solution must be employed based on interferometric subtraction of the dropped subchannel.

Reference [62] reported on an add/drop module based on an opto-electronic interferometer structure allowing the extraction of individual sub-carriers from Nyquist-WDM and CO-OFDM superchannels, as well as the insertion of sub-carriers into existing superchannels, through intradyne conversion of the optical signal to digital electronic baseband, followed by digital electronic signal processing and subsequent electro-optic conversion. The performance was assessed via simulations to identify its system sensitivities, as proper erasure critically depends on destructive optical field superposition. An alternative opto-electronic substitution technique based on frequency conversion in a nonlinear fiber was experimentally demonstrated for OFDM sub-carriers [63], with the detection and opposing signal generation performed off-line.

All-optical OFDM subcarrier extraction can be substituted for the opto-electronic approach for generating the cancelling subchannel of the interferometer, in a technique called terabit interferometric drop-erase-add (TIDE) multiplexing for superchannels [64]. Starting with a copy of a superchannel containing the subchannel to be dropped, an optical FFT is performed for filtering the OFDM subcarrier [65], followed by temporal sampling with an optical gating function and reshaping the sampled signal to an OFDM subcarrier with a subsequent optical FFT filter. The two paths are recombined with appropriate phase, time, power, and polarization alignment so that the subchannel to be dropped is interferometrically suppressed from the superchannel, at which frequency a new subchannel can be added. An experimental demonstration of the all-optical TIDE architecture operating in real-time for BPSK and QPSK CO-OFDM superchannels was reported in [66].

Whether all-optical or opto-electronic techniques are used for optical add/drop of spectrally overlapping subchannels from a superchannel, the customized hardware can be deployed in a two-tiered hierarchical ROADM architecture, as shown in Fig. 11, replacing the HSR filter with the interferometric arrangement.

IV. ROADM Functionality for SDM–WDM Networks

Elastic optical networking and future advances such as subchannel add/drop capability allow the full and efficient utilization of the optical transmission bandwidth spanned by the communication system. Once that communication band is exhausted, other means for supporting additional capacity must be introduced. One of the leading candidates offering a significant capacity multiplier is SDM, introduced via new fiber types offering additional conduits of information channels such as spatial modes or cores. Expanding fiber link channel counts to the spatial domain requires further innovation and flexibility to route these channels at network nodes. We discuss SDM–WDM ROADM functionality and additional photonic-switching innovations in support of the spatial domain in this section.

A. SDM–WDM Switching Strategies

Previous ROADM solutions provided flexibility across the wavelength domain, enabling the switching of wavelength channels (down to the subchannel granularity). Employing both WDM and SDM within fiber links expands the channel count M-fold, with M being the number of spatial modes or cores. However, whereas wavelength

channels do not intermix in a linear medium, spatial channels might. When spatial channels intermix, the information can still be unraveled by employing multiple input, multiple output (MIMO) signal processing across the mixed channels. For MIMO processing to function, all the mixed channels have to be present and jointly processed. Hence, when mixing occurs, the mixed channels must be kept as a group and cannot be independently switched to a distinct network destination. We distinguish between three mixing situations influencing the switching strategies: (1) *no spatial mixing*, when cores are isolated or several single-mode fibers are used to create a spatial group, (2) *mixing between all spatial modes*, which may occur in multimode fibers or in fibers with coupled cores, and (3) *mixing within subgroups*, which may occur in few-mode, multi-core fibers or irregularly spaced multi-core fibers. With these mixing situations under consideration, we identify four main SDM–WDM switching strategies, categorized according to the switching granularity (i.e., the smallest switched element) [67]:

1) Space Granularity: Switching is performed in the spatial domain across the entire optical communication band (all WDM channels), forfeiting any wavelength flexibility. The switching hardware is devoid of any dispersing means, thus relying on relatively simple space switches. This switching strategy is only applicable to the no spatial mixing transmission case.

2) Space–Wavelength Granularity: Switching can be prescribed down to the single spatial and wavelength channel granularities in the fiber, exploiting the full switching potential of an SDM–WDM transmission system. Due to its offered finest granularity (resulting in greatest flexibility), its potential implementations are the most cumbersome. As in the space granularity case, space–wavelength granularity requires that the spatial modes/cores do not mix.

3) Wavelength Granularity: Contrary to space granularity, which forfeited access to the spectral domain, wavelength granularity sacrifices the spatial domain in order to simplify the switching hardware. Implementations rely on modified WSSs in support of joint switching of all M spatial channels on a wavelength basis. This scenario is the only one applicable when all the modes/cores intermix, as they must remain together as a group throughout the network.

4) Fractional Space, Full Wavelength Granularity: For fibers where mixing is limited within spatial subgroups, this strategy adopts the wavelength granularity approach to the subgroups, and each subgroup can be independently switched on a wavelength basis. Attractive features of this strategy are the intermediate routing flexibility and moderate implementation complexity.

Possible implementations for the four switching strategies are shown in Fig. 13 (non-exhaustive) and detailed in the next subsection. While these switching strategies are geared for different mixing situations experienced in fiber transmission, the more restrictive solutions can always be applied to the less restrictive ones. For example, the wavelength granularity and fractional space–wavelength granularity approaches can be adopted for transmission systems having no spatial mode/core mixing. In addition, for fibers having no spatial mixing, the switching may offer the ability to switch a wavelength channel from one spatial mode/core on an ingress fiber to a different one at the egress fiber. This SDM "lane change" can be used to circumvent some blocking situations, and can be recognized as the equivalent of "wavelength conversion" in WDM networking, which has been extensively investigated in the past for resolving blocking cases [68]. However, whereas SDM lane changes can be performed with simple passive optical switches and are an attractive networking feature, wavelength conversion requires more complicated solutions that have not been adopted in commercial WDM systems.

B. SDM–WDM ROADM Architectures

Implementing the different SDM–WDM ROADM nodes can be accomplished through many of the technologies that have been developed for SMF, as well as some complementary ones. Foremost of the latter is a spatial multiplexer (demultiplexer), which is used for combining (separating) M input (output) single-mode channels into (out of) an SDM fiber, ideally in a one-to-one mapping between mode/core and individual SMF. Employing such SDM demultiplexers (demux) at the ingress ROADM ports separates out the spatial channels to a discrete SMF set for subsequent switching.

1) Space Granularity Architecture: Considering the space granularity approach, fiber switches are then required to route the entire communication band on each separated spatial channel to its destination. Two switching scenarios can be considered: (1) routing from an ingress spatial channel (core or mode) is performed on the same spatial channel on the egress fiber, i.e., without spatial lane change, and (2) unrestricted routing is performed permitting spatial lane changes. Switching without lane changes can be realized by a bank of small OXCs, one per spatial channel [Fig. 13(A)]. The input/output port count of an individual OXC (devoted to a spatial channel) is at minimum the number of directions, D, i.e., $D \times D$ OXCs, and M such OXCs are required. (Additional OXC ports may be desired in support of local add/drop.) In support of lane changes, one large OXC should handle all the node traffic [Fig. 13(B)]. In this case, the OXC port count is $(D \cdot M) \times (D \cdot M)$ (again, at minimum). A significant risk associated with an architecture based on a single large OXC is its failure impact. This can be circumvented by a second OXC placed in parallel for protection, but this adversely impacts the cost, space requirement, and fiber-routing complexity. Without lane changes using a bank of smaller OXCs, a single switch failure impacts only $1/M$ of the node traffic.

2) Space–Wavelength Granularity Architecture: Space–wavelength granularity offers the finest switching granularity at the expense of implementation complexity. Here, too, lane changes may be supported at the cost of additional complexity. Access to the space–wavelength granularity is achieved by first spatially demultiplexing the signal,

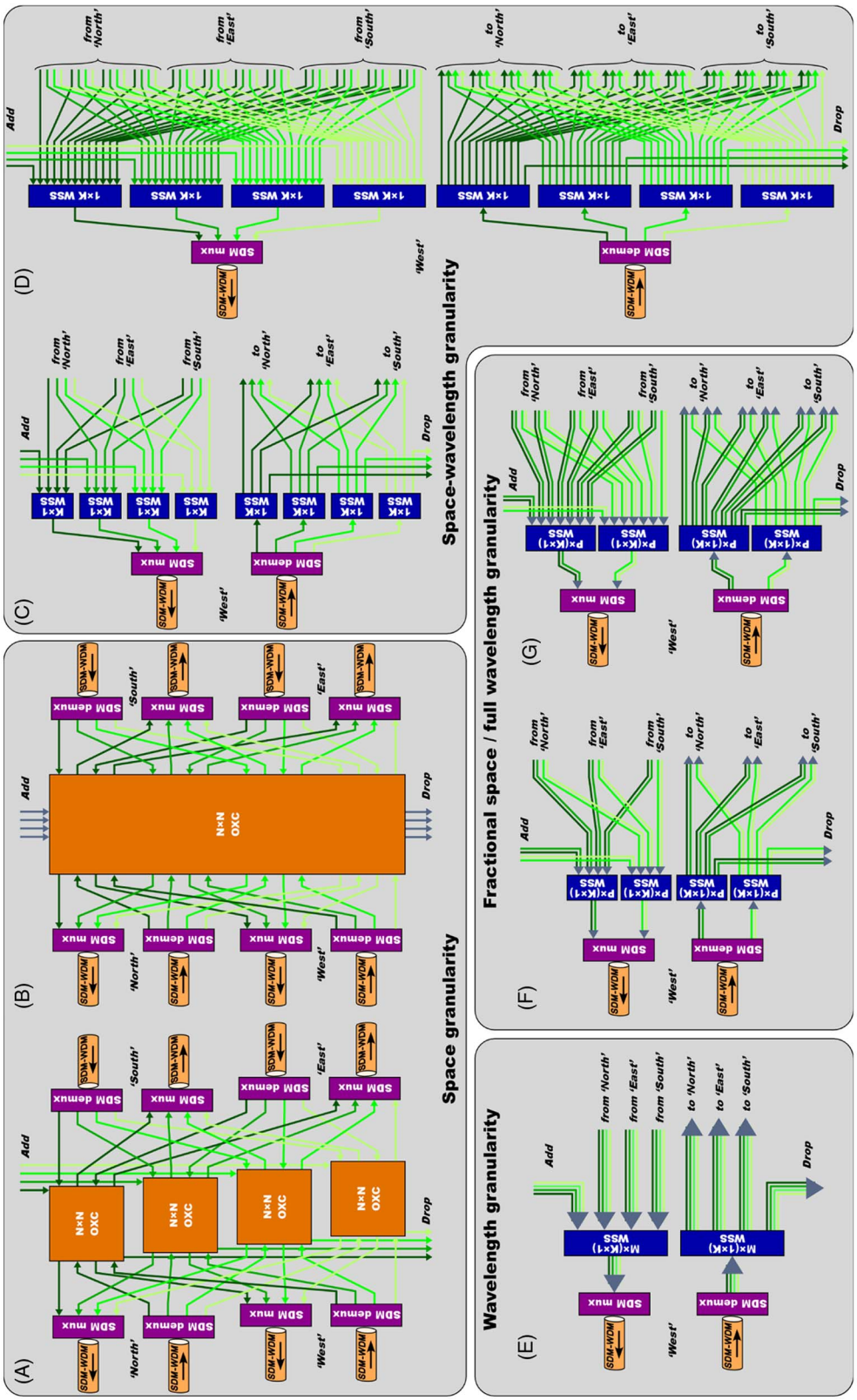

Fig. 13. Proposed implementations of SDM–WDM switching strategies for different switching granularities, drawn for four spatial modes and a degree-four node. (A) Space granularity without SDM lane changes. (B) Space granularity with SDM lane changes. (C) Space–wavelength granularity without SDM lane changes. (D) Space–wavelength granularity with SDM lane changes. (E) Wavelength granularity. (F) Fractional space and full-wavelength granularity without lane changes. (G) Fractional space and full-wavelength granularity with lane changes. Cases (C)–(G) show the switching hardware for one direction only (West).

followed by placing a WSS on each spatially separated channel for routing to other egress ports. If routing to the same spatial channel on the other ports, then the number of WSS output ports needs to be D, with routing to $D-1$ other destinations and at least one drop port [Fig. 13(C), with only one direction shown for simplicity]. If spatial lane change is desired, then each ingress WSS should reach all other destinations and spatial channels, requiring the WSS to support $M \cdot (D-1)$ + drop output ports [Fig. 13(D)]. The fiber wiring can become unwieldly in this case.

An implementation alternative for the cross-connect functionality provided by the route-and-select topology can be obtained by placement of a transparent optical cross-connect switch, as has been envisioned early in the WDM era [69]. For space–wavelength granularity, each fiber would need to be demultiplexed twice, per space and wavelength domains. However, such a solution would lose the flexible bandwidth assignments and EON support. In addition, it would require an OXC per wavelength channel. Hence, it cannot meet the modern networking requirements, demands a large switching gear count, and presents a severe wiring problem. Thus, we do not foresee such a solution as a viable alternative.

3) Wavelength Granularity Architecture: Implementation simplicity can be obtained by sacrificing flexibility, as has been the case for space granularity. In wavelength granularity, all spatial channels are routed as a whole per wavelength channel. This functionality can be provided by a single WSS modified to support joint switching over all SDM channels on a wavelength basis by employing spatial diversity [Fig. 13(E)]. In the particular case of a few mode fiber (FMF), joint switching within the WSS can be implemented without requiring spatial diversity and its associated space mux/demux, providing further implementation simplicity. Such joint-switching WSSs are described in the next subsection discussing new technologies.

4) Fractional Space–Wavelength Granularity Architecture: As a compromise between switching granularity size and implementation complexity and cost, the joint-switching concept of spatial channels can be applied to subgroups of the spatial channel count. Hence, if the M spatial channels are divided into subgroups of size P, then the number of WSSs required to route subgroups is M/P (which is obviously bounded between the cases of wavelength granularity and space–wavelength granularity). This fractional space, full wavelength granularity solution can be implemented without lane changes (or rather subgroup change), see Fig. 13(F), or with lane changes, Fig. 13(G). The latter, while indeed more cumbersome, is more tolerable if the subgroup count, M/P, is a small number.

5) Architecture Comparison: To better gauge the scaling of the SDM–WDM ROADM solutions just outlined, we demonstrate the implementation possibilities using reasonable values for the node degree and spatial channel count in a hypothetical WDM-SDM network. Let us assume that $D = 4$ to cover the most prevalent network node degree size, and that the SDM channel count is $M = 12$ (for an order of magnitude capacity increase). We further assume that the 12 spatial channels can be separated out into four groups of size $P = 3$ (perhaps a four-core fiber, where each core supports three modes), though other options can be considered. The hardware required for the implementation is tabulated in Table I.

It becomes immediately apparent that the technologies required to implement the network node architectures are available or have been demonstrated (as outlined in the next section), and that many WSSs will be required in support of the SDM–WDM switching. We generalize the node-switching requirements and summarize the attributes of each of the SDM-switching strategies and enabling ROADM architectures just described in Table II. Advantageous attributes are shaded green, disadvantageous in red, and neutral in yellow. While ideally it is desirable to switch at the smallest granularity, this is not always possible (if modes are mixed), and it comes at a cost premium. Hence, the architectural choice is a multi-variable optimization problem that needs to take into account the physical-level impairments.

Based on this discussion, it should be clear that the choice of switching granularity directly affects the specific SDM–WDM ROADM architecture, routing algorithms, and related network performance. For instance, for wavelength granularity (strictly required for a MIMO-based SDM system with mixing [70,71]), a spatial superchannel will occupy all the M spatial modes for a given wavelength slot. While this constraint on the creation of spatial superchannels will limit the flexibility to switch, add, and drop single SDM channels, it simplifies the network control and provisioning since, for instance, fragmentation will be limited to the wavelength domain only. In the case of an SDM system not exhibiting mixing among its spatial channels, fractional-space, full-wavelength granularity or wavelength granularity switching can still be used so as to take advantage of its implementation simplicity and cost benefits. However, fragmentation in both the spatial and wavelength domains

TABLE I
SWITCHING HARDWARE FOR A NETWORK NODE OF DEGREE 4 AND SPATIAL CHANNEL COUNT OF 12

Architecture	Switched Granularity	Switching HW
Space granularity with lane changes	Entire commun. band per spatial mode	Single 48 × 48 OXC
Space–wavelength w.o. lane changes	Entire commun. band per spatial mode	12 units of 4 × 4 OXC
Space–wavelength with lane changes	Wavelength channel per spatial mode	24 units of 1 × 37 WSSs per direction, 96 total
Space–wavelength w.o. lane changes	Wavelength channel per spatial mode	24 units of 1 × 4 WSSs per direction, 96 total
Wavelength granularity	All spatial modes per wavelength channel	8 12 × (1 × 4) WSSs (2 per direction)
Fractional space, with lane changes	Group of three modes, per wavelength	32 units of 3 × (1 × 13) WSSs
Fractional space, w.o. lane changes	Group of three modes, per wavelength	32 units of 3 × (1 × 4) WSSs

TABLE II
COMPARISON BETWEEN SDM–WDM SWITCHING STRATEGIES (ADAPTED FROM [65])

	Space-wavelength granularity	Space granularity	Wavelength granularity	Fractional space, full wavelength granularity
Minimum switching granularity	Single WDM channel on a single spatial mode.	Entire optical communication band on a single spatial mode.	Single WDM channel across all spatial modes.	Single WDM channel over subset of spatial modes.
Realization	No lane change: 2M WSSs per direction with D I/O ports at minimum (to support at least one A/D port). With lane changes: 2M WSSs per direction with M·(D-1)+1 I/O ports at minimum (to support at least one A/D port).	No lane change: M OXC with D×D port count (at minimum, and additional ports for local A/D). With lane change: One large OXC with (D·M)×(D·M) port count (at minimum, and additional ports for local A/D).	Two high-port-count joint switching WSS per direction configured as an M×(1×D) WSS applied to all spatial modes in parallel.	No subgroup lane change: 2M/P high-port-count joint switching WSS configured as P×(1×D) WSS applied in parallel to all spatial modes in a subgroup. With subgroup lane change: 2M/P high-port-count joint switching WSS configured as P×(1×[(D-1)·M/P+1]) WSS.
Flexibility	Each mode/WDM channel independently provisioned and routed. Spatial mode maintained. Prone to wavelength contention.	The complete optical communication band is routed across network. Coarse granularity. If WDM channels need to be extracted then WSS need to be introduced.	Each spatial superchannel provisioned across all modes. Susceptible to wavelength contention. Add/drop bound to direction unless MCS technology expanded.	Compromise solution using small SDM groups. More efficient when provisioning low capacity demands.
Scaling	Switching node cost linearly scales with capacity, not providing the price benefit essential for SDM adoption. Integrated WSS array would help suppress the cost increase.	OXC supports foreseeable mode and fiber counts, but is single point of failure. Without lane changes (using several smaller OXC), failure impacts only 1/M of traffic. Pricing favorable but when wavelength add/drop required, needs WSS modules.	Cost roughly independent of SDM count. Inefficient for low capacity connections due to minimum BW provisioned across SDM. Large SDM Rx/Tx are integration and DSP challenge.	Cost scales as group count. Groups can be turned on as capacity grows, offering pay-as-you-go alternative. Maintaining small group sizes facilitates MIMO processing at Rx.
Estimated loss	10 dB per I/O fiber link. For MCF or FMF transmission fiber, extra 4 dB loss is induced by the spatial MUX/DEMUX	3 dB per I/O fiber link being switched. If add/drop from SDM fiber is extracted, 10 dB excess loss for through. For MCF or FMF transmission fiber, extra 4 dB loss is induced by the spatial MUX/DEMUX	10 dB per I/O fiber link. For MCF or FMF transmission fiber, extra 4 dB loss is induced by the spatial MUX/DEMUX	10 dB per I/O fiber link. For MCF or FMF transmission fiber, extra 4 dB loss is induced by the spatial MUX/DEMUX

might occur. It becomes then necessary to study new routing and defragmentation algorithms that take into account this new spatial dimension. While the discussion of the different routing algorithms and strategies goes beyond the scope of this paper, the reader can refer to [14,16,72–75] for more details.

C. Technology Advances Supporting SDM–WDM Switching

The various SDM–WDM ROADM realizations which are required for implementation of transparent optical networks with unprecedented capacity make use of ancillary photonic innovations for multiplexing and switching (fiber amplifiers in support of SDM are beyond the scope of this paper). It is imperative that these innovations in support of the SDM capacity multiplier be more economical than achieving the same capacity increases by deploying additional SMF systems in parallel. This is only possible via integration technologies incorporating the spatial degree of freedom.

1) Spatial Multiplexer: As noted earlier, many of the ROADM designs make use of elements developed originally for SMF-based systems. When utilized for SDM systems, they must be preceded/followed by a spatial demultiplexer/multiplexer whose role is to convert between the M cores or modes of the SDM fiber and M separate SMFs. Ultrafast laser inscription (ULI) can be utilized to inscribe waveguides in three-dimensional space (under programmatic control) inside a glass block, based on permanent nonlinear densification of the glass at the focal region of the inscribing beam (Fig. 14, top). The written waveguides can be made with mode sizes similar to SMF for efficient edge coupling. 3D ULI waveguides can serve to interface between an SMF array and the cores

of a multi-core fiber (MCF), thereby establishing a one-to-one mapping between cores and individual SMFs (sometimes referred to as MCF fan-out or break-out). If the MCF contains well-isolated cores (no coupling between them), then an SDM link composed of a multiplexer, MCF, and demultiplexer will not exhibit mixing, enabling the space and space–wavelength granularity SDM–WDM ROADM solutions. For mode-division multiplexed transmission, the ULI waveguides can be designed to excite spatial modes by bringing them close to each other, such that they begin to mutually couple, while adiabatically reducing the waveguides' size and pitch. As the individual waveguide modes expand (due to the decreasing core sizes), the array structure starts to guide supermodes. It is the design goal to have the supermodes match the mode structure of the few-mode fiber, with the formed transition structure called a photonic lantern (PL). When designed well, the PL can serve as a lossless mapping between M fiber modes and M separate SMFs.

While a PL can efficiently interface between FMF and the SMF array, they do not necessarily maintain a one-to-one mapping between modes and individual SMF. A PL can be designed with varying degrees of mode-selectivity, including full selectivity (having a diagonal transfer matrix between modes and individual SMF, or a one-to-one relationship), mode-group selectivity, and no mode selectivity (where each SMF excites all modes with different efficiencies; see Fig. 14, center). Fully selective PLs are hardest to fabricate and tend to have high losses and are limited to a small number of modes, whereas completely scrambling PLs are simpler to fabricate, have lower losses, and can scale to higher numbers of modes. The mode scrambling is not perceived as a limitation, as over long transmission distances (several hundreds of km), the modes become strongly mixed anyway and require MIMO processing to undo the mixing at the SDM receiver. The PL-induced mixing is taken out just as well by the MIMO processing. Mode-selective PLs are useful in short-length propagation (<40 km), where mixing occurs between fiber modes falling within the same mode group (having very similar propagation constants, delays, mode areas, and similar gains in amplifiers). Mode-selective and mode-group-selective PLs can be used to compensate for the differential group delay (DGD) of fiber spans or the modal gain differences in fiber amplifiers [76].

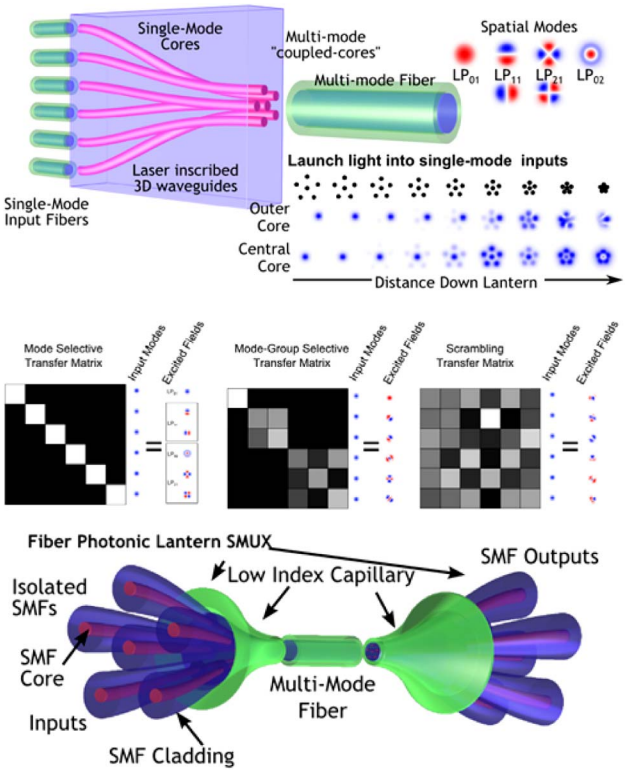

Fig. 14. Spatial mode demultiplexer between a multimode fiber and SMF array based on a PL. Top: PL written by ultrafast laser inscription. Center: Transfer matrix characteristics between modes and individual SMF for mode selective, mode-group selective, and scrambling PL. Bottom: PL made by fiber tapering.

PLs can also be fabricated using fibers, as an alternative to the 3D ULI approach. Multiple fibers are placed within a low-index capillary, and the structure is tapered until the light is guided by the fiber cladding and low-index capillary rather than by the individual fiber cores [77] (Fig. 14, bottom). The fiber PL is also an adiabatic device, has low loss, can be spliced directly to the FMF, and can be scaled to a large number of modes. When identical fibers are used, the fiber PL has no mode-selectivity (i.e., a scrambling transfer matrix). To add mode selectivity, fibers with different core sizes can be used. Mode-group-selective devices have been demonstrated with up to 15 spatial modes, enabling transmission in fibers supporting 10 and 15 modes [78–80]. Drawbacks of the ULI PL compared to the fiber version are higher insertion loss, difficulty in forming very large multimode regions, and achieving a high NA.

2) Multiple WSS Packing: One of the detriments of SDM–WDM ROADM designs in support of space–wavelength granularity is their need for many WSS modules in their realization, resulting in an unfavorable cost basis that scales with the mode count. Having multiple, co-packaged WSSs within a single sub-system, sharing the same optical, optoelectronic, electronic, and software control elements can alleviate this largest disadvantage. The SPOC-based processing front end within a free-space WSS can be designed to support such functionality (see Fig. 15). Here, the SPOC device implements an identical spatial beam transformer at each zero-diffraction-order WGR having multiple input/output waveguides at offset positions to the slab lens. The offset positions lead to broadened beams emerging from the WGR, with each offset position corresponding to a unique tilt angle. The subsequent free-space optical arrangement maps each tilt to a unique offset position on the LCoS SLM. The center WGR serves as the input (shown with three inputs A_{in}, B_{in}, and C_{in}), which strike the LCoS SLM at unique positions (A, B, C). The LCoS SLM directs the wavelength channel from each independent WSS to its designated direction, and the remaining WGRs serve the different output fiber ports (shown at the top output port position). The WGRs perform the function of angular multiplexing, allowing each spatially separated WSS to act independently, with its own input and output fiber ports that do not intermix. The spatial

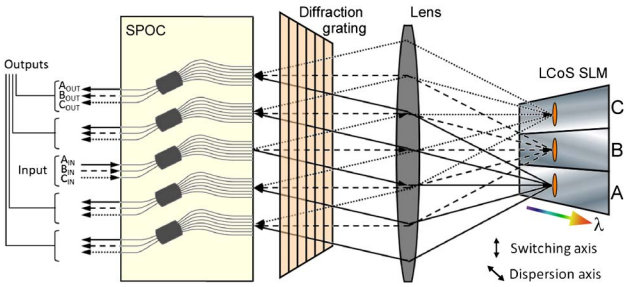

Fig. 15. WSS multiplexing with a SPOC front end. Three 1×4 WSSs are integrated. The light paths of WSS_A, WSS_B, and WSS_C are shown by solid, broken, and dotted lines, respectively.

overlap of the light paths among the WSSs makes the module small, and the optical setup is as simple as that of a conventional $1 \times K$ WSS by sharing the common optical components. This multiple WSS packing is thus nearly identical to the SPOC-based $D \times L$ WSS (Fig. 5), but without the selector switches on the output fibers [81]. The SPOC front end can be interfaced to SDM fibers using ULI waveguides in a glass block interface, as has been demonstrated for MCF integration [82].

3) Joint Switching WSS: Another approach for reducing the SDM-ROADM hardware count and implementation cost is to employ WSSs supporting the joint-switching mode of operation, required for the wavelength-switching granularity approach. A joint-switching WSS accepts all the spatial channels and switches them as a group, on a wavelength-channel basis, to desired output SDM destinations. As previously noted, the design of a conventional WSS has all the fiber ports dispersed and imaged to the same positions at the switching plane, where the input beam is directed toward a desired output fiber on a wavelength basis (see Subsection II.A). Since all the fibers are imaged to the same position, the beam steering can simultaneously redirect multiple beams incident on it, with all beams experiencing the same beam-steering shift. If the WSS input/output fibers are arranged in a regularly spaced array, then the steering of a set of inputs is reimaged onto different sets of outputs. Associating the groups of fibers with SDM fiber interfaces allows the switching of all the spatial channels to their destinations, gaining the SDM capacity multiplier without increasing the WSS count (same WSS count as SMF implementations). This spatial diversity technique reformats the channels of the SDM fiber to spatially separated and parallel beams, enabling their joint switching with the same hardware complexity as the SMF-based WSS. The joint-switching concept was first demonstrated with MCF interfaces with seven cores [12]. The cores were separated by an MCF breakout device and attached to the WSS. Two other sets of seven fibers were each attached to the output SDM fibers (Fig. 16, top). This enables switching the seven spatial channels to one of two output destinations, for a $7 \times (1 \times 2)$ WSS functionality. This WSS requires 21 SMF at its interfaces, and indeed was based on a conventional 1×20 WSS with fiber port reassignments. The same joint-switching concept was subsequently demonstrated for FMF, replacing the external MCF breakout devices with

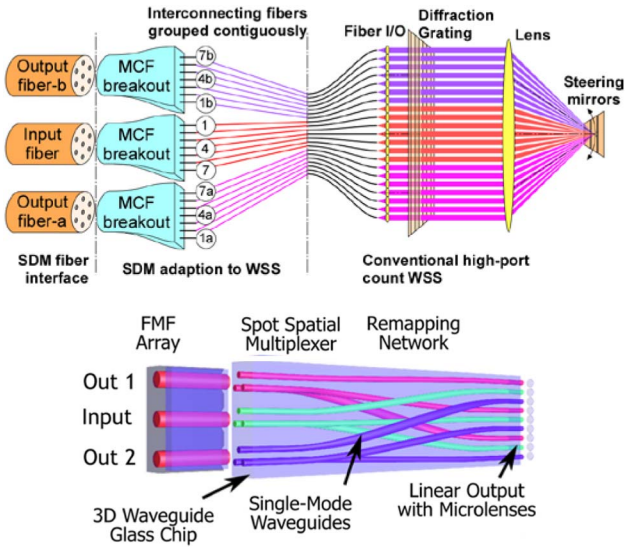

Fig. 16. Top: WSS adapted by spatial diversity for joint-switching operation. SDM fibers (MCF shown, but other SDM solutions supported) are spatially demultiplexed and attached to the SMF ports of the WSS. Bottom: Joint switching with space demux (using 3D waveguides) integrated within WSSs, for FMF WSSs supporting three spatial modes.

FMF demux (three modes) and interfacing the SMF to a commercial dual 1×20 WSS [83]. Alternatively, the mode demux can be integrated within the WSS module, as demonstrated in [84]. Spatial diversity was obtained from a 3D waveguide front end, which demultiplexes the modes from three mode fibers and places them in linear array form in the steering direction, but also reshuffles the beams such that the steering angle requirement for switching is reduced (Fig. 16, bottom).

These joint-switching WSS solutions based on spatial diversity reduce the number of supported output SDM destinations by the spatial channel count, as exemplified by the 1×20 WSS turned into a $7 \times (1 \times 2)$ WSS. Thus instead of having 20 output port options (in support of network routing and add/drop support), functionality is reduced to two output ports only (add and drop node). Two techniques have been demonstrated to address this limitation: a spatial diversity WSS that maps the fiber ports to two dimensions and a WSS without spatial diversity that steers multimode beams and maintains port count.

Since a WSS images and disperses parallel beams at the lens back focal plane where beam steering occurs, the spatial diversity can be extended beyond one-dimensional realizations. By mapping the spatial channels to a 2D array form while keeping the switching direction in the vertical direction, switching action can be applied to rows of fibers of the array (Fig. 17). If SDM groups are associated with rows of the 2D array and an input SDM fiber is spatially demultiplexed and fed to one row, then the entire SDM group can be jointly switched to output SDM fibers associated with other rows. If an SDM group size is larger than the column count, then multiple rows can be associated with each SDM group. In [85], a 19×3 single-mode fiber array (57 fibers) fed the WSS structure, which can support

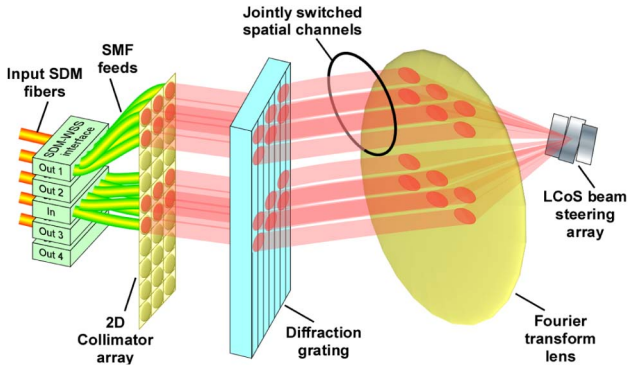

Fig. 17. SDM WSS with spatial diversity spanning two dimensions. Spatial channels are remapped to rows of the array, and switching is performed in the vertical direction. Input row(s) steered to desired output row(s).

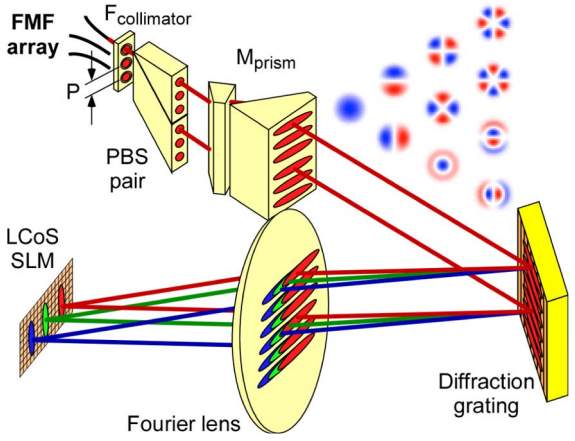

Fig. 18. FMF WSS with multimode beams propagated and steered within the WSS.

$3 \times (1 \times 18)$ switching functionality, demonstrating that an SDM-WSS can be designed for joint switching of SDM channels to many output destinations using spatial diversity. Since the spatial demultiplexers are external to the WSS, it can be mated to any SDM fiber solution. In Ref. [85], the WSS was utilized in the first ROADM node realization within a heterogeneous network. Different SDM fibers supporting six spatial channels were deployed between four nodes of a line system (links with six SMFs directly interfaced to the WSS, six-mode FMF with fiber PL spatial demux, and six-mode MCF using a tapered fiber bundle spatial breakout). At the SDM ROADM node, the spatial channels were separated and jointly switched with the 2D WSS (wavelength granularity approach as the channels experienced mixing in fiber transmission). SDM groups were mapped to two rows of the 19×3 fiber array (since the 2D fiber array had three columns), with the WSS then providing $6 \times (1 \times 8)$ functionality (one row was discarded due to the odd row count). The WSS spectral responses were nearly identical for each spatial channel due to the spatial diversity solution.

Spatial diversity solutions require the WSS optics to handle many more free-space beams than switching ports, due to the spatial multiplier. This strains the optical design of the WSS (performance and size). For FMF-based systems, the fibers can be directly interfaced to the WSS foregoing demultiplexing and spatial diversity. The beams within the WSS become multimode, but otherwise traverse the same optical elements as a conventional WSS. The number of free-space beams within the WSS equals the number of switching ports (Fig. 18). However, the spatial mode structure of the beams impacts the spectral channel characteristics. At the beam-steering plane, where the beams are spatially dispersed, flexible channel extent is defined by the LCoS SLM. Beam modes of optical frequencies that strike the channel edges experience clipping, which impacts each mode differently and disrupts mode orthogonality (resulting in mode-dependent passbands and spectrally dependent mode mixing at channel edges). This leads to larger spectral transition bandwidth between the pass-band and the block-band. Hence, larger guard bands are required between adjacent wavelength channels, impacting the spectral utilization of the communication band. Conversely, higher spectral resolution optics can be employed to achieve conforming transition bands. An alternative FMF–WSS implementation that addresses the channel passbands could be obtained if rectangular core fiber (single-mode in one dimension, multimode in the other) were used for transmission instead of circular core fiber.

A FMF–WSS was demonstrated with 10 fiber ports, where each I/O fiber supported three spatial modes (LP_{01} and the degenerate LP_{11} modes), for $3 \times (1 \times 9)$ WSS functionality, and was used in a three-mode transmission experiment over 300 km, where the WSS was passed up to ten times within a recirculating loop [13,86].

V. Cost Evaluation of ROADM Architectures For Transmission Options Beyond the C-Band

We next attempt to compare the costs of different architecture options in support of capacity extending beyond the single-mode communication band. This will be somewhat speculative because most of the components have not yet been commercialized and their cost established. However, we can make some comparisons with existing products. For example, a 1×5 joint-switching WSS for seven-core fiber, or a $7 \times (1 \times 5)$ WSS (with a total of 42 ports), would be about the same size and complexity as a conventional 1×41 WSS, a product which does not yet exist. Since its port count is equal to that of a Twin 1×20 WSS, their cost should be roughly equivalent. We can extrapolate to higher-port-count devices by comparing the relative costs to lower-port-count devices. However, we do not venture too far off in our extrapolation (i.e., we look at SDM increases of up to factor 7), as it becomes increasingly speculative to estimate the cost of devices with port counts farther beyond those of currently manufacturable devices. We consider only the costs of the ROADM components, namely the WSSs, MCSs, and amplifiers associated with the MCSs. The remaining network components (fiber, line amplifiers, transceivers, etc.) are assumed to be cost neutral for different architectures, which may not always be true due to

co-packaging cost benefits, but we have insufficient information at this point to compare them; hence, they are excluded from the analysis.

As a baseline, we choose a route-and-select CDC-Flex ROADM node architecture using WSSs and MCSs in support of four network directions, as shown in Fig. 19. The baseline system has a total of four Twin 1 × 10 WSSs (one Twin switch per direction), two Twin 4 × 16 MCSs (two MCSs for add and two MCSs for drop, which can be used in protection mode, i.e., no single point of failure for add/drop channels, or in support of higher add/drop channel counts), and 16 amplifiers associated with the MCSs to compensate for their splitter/combiner losses. As protection schemes are beyond the scope of this paper, we use the available add/drop ports to support a total of 32 flexible channels. When the node capacity is scaled upward in this study, we also scale the add/drop channel capacity in the same proportion. When comparing costs, we calculate the relative cost per bit, so for example, if the capacity is increased by a factor of 7, we divide the total ROADM cost by a factor of 7 to achieve a relative cost-per-bit basis. The cost model we employ is comparative, with the Twin 1 × 10 WSS costing one unit, the relative cost of the Twin 4 × 16 MCS module being 0.68, and the cost of a booster amplifier being 0.08. The total cost of the baseline single-mode system of Fig. 19 (four Twin 1 × 10 WSSs, two Twin 4 × 16 MCSs, and 16 amplifiers) is normalized to one. In considering device capability for higher port counts, we assume a 50% price increase for a WSS (toward Twin 1 × 20 WSS) and 25% increase for an MCS (toward Twin 8 × 16 MCS).

We consider the following capacity expansion options: A. single-mode fiber overlays, which can be implemented (i) with independent channel routing with SDM lane changes or (ii) without, in which case the cost per bit is essentially the same as the baseline since all elements are simply replicated, or (iii) with joint-switching WSSs; B. few-mode fiber; C. multi-core fiber; and D. extension to L-band and S-band. In each case, where appropriate, we consider a moderate (×3) capacity expansion (which could also be achieved by spectral extension and compared against three-mode FMF) and larger (×7) capacity expansion (for comparison against seven-core fiber).

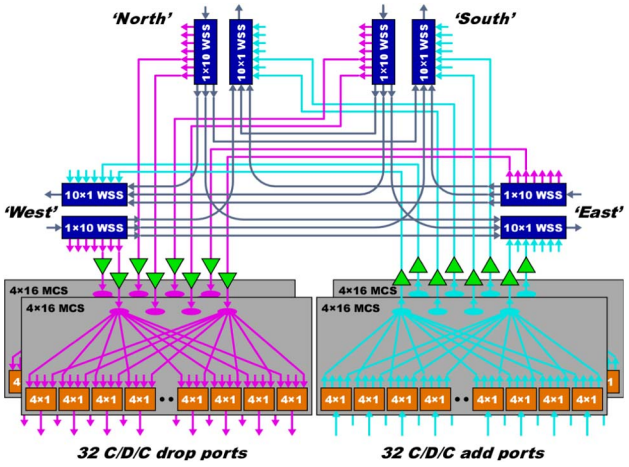

Fig. 19. Baseline ROADM node architecture used for the cost analysis.

A. Single-Mode Fiber Overlays

The first capacity expansion option we consider is single-mode fiber overlays with SDM lane changes. The overlay fibers are treated as additional node degrees except for the option to switch back to the same direction, which is not supported or needed. With no mode mixing present, this scheme can support independent switching with space–wavelength granularity for each overlay fiber. This could be considered the default expansion option because it requires no new technology development (at least for small numbers of overlay fibers) and is being implemented today for overloaded links. However, fiber overlays lead to increasing cost per bit because not only are more WSSs and MCSs required, but those components must be upgraded to support more ports. We consider only WSS options that do not exceed the beam-steering capabilities of currently available technology. For the MCS, its complexity scales as the product of the number of common ports and A/D ports. This product represents the worst-case number of MCS waveguide crossings; each A/D port has a selector switch for connecting to one of the common ports; the number of A/D ports determines the splitting ratio, and hence the inherent loss to each common input port. The number of common ports must equal the degree of the node for unconstrained access; hence, as more overlay fibers are added, the number of common ports on each MCS increases. We assume that the complexity of each MCS cannot increase without bound. Hence, we limit the complexity by proportionally reducing the number of A/D ports when the common ports increase in an effort to achieve a manufacturable product (using the 8 × 16 MCS as the state of the art scaling). This caps the cost and complexity to that of existing 8 × 16 MCSs, but increases the number of MCSs required and the number of WSS ports for connecting to the MCS modules.

Using these scaling assumptions, we arrive at a total WSS cost of 4.4 times the baseline WSS cost for a 3× overlay (three fibers in each of the four directions, requiring by 12 units of Twin 1 × 20 WSSs), and 25.5 times the baseline WSS cost for a 7× overlay (56 units of 1 × 80 WSSs), and a total MCS cost of 5.7 times the baseline MCS cost for a 3× overlay (9 units of Twin 12 × 11 MCSs) and 31 times the baseline MCS cost for a 7× overlay (49 units of Twin 28 × 5 MCSs). A total of 216 amplifiers are required for the 3× overlay (9 MCSs ×12 common ports ×2 for add and drop), but it is noted that for the 7× overlay case, the number of A/D ports on each MCS is quite small (and hence the splitting ratio within the MCS is low), so we assume that amplifiers are not needed. Had amplifiers been required, the 7× overlay configuration would have required more than 2000 amplifiers, which would have had a detrimental impact on the overall cost. As an aside, consider that a 28 × 16 MCS could be manufactured; the overall cost of the 7× overlay using this hypothetical MCS variant would have comparable or possibly higher cost than using the 28 × 5 MCS, as the cost benefits of reducing

the number of MCS modules and WSS port counts would be offset by additional amplifier costs. In any case, it is apparent that the ROADM costs for fiber overlays increase faster than the capacity increases.

In consideration of single-mode fibers without SDM lane changes, which is essentially M independent baseline networks, this arrangement would enable capacity increase with the same cost per bit as the baseline system. While this would result in lower cost compared to the aforementioned system supporting SDM lane changes, the cost advantage can only be realized if every link of the network requires M times the capacity. At present, adding overlays as node degrees is the preferred expansion option because capacity growth is uneven throughout the network and the routing flexibility of SDM lane changes enables efficient use of existing hardware. However, this could change in the future as the number of overlays increases.

B. Few-Mode Fiber Systems

For FMF, we assume the ROADM architecture looks the same as that shown in Fig. 19 (same number of components with similar port counts) but with all components made compatible for FMF. Our task here is to estimate the cost of these FMF-compatible components. For a FMF WSS we choose the spatial diversity approach (as shown in Fig. 17) rather than propagating multimode beams (see Fig. 18), due to similar spectral resolution requirements, facilitating the cost comparisons to existing SMF WSSs. Here, we assume the separated modes are mapped to fibers that are grouped together (without port reshuffling). These fiber ports can be spaced more tightly than conventional WSS ports, as crosstalk between modes of the same fiber is insignificant, thereby reducing optics height and steering angle requirements and hence reducing the cost of the WSS. For example, a 1×10 WSS for three-mode FMF with compressed spacing between ports from the same fiber would require about the same optics height and beam steering requirements as a 1×20 WSS for SMF, even though there are effectively 30 output ports. Thus, the WSS cost is estimated to be about the same as the cost difference between a 1×10 WSS and a 1×20 WSS for SMF, a factor of about 1.5. Similarly, the WSS cost is estimated to increase by a factor of 1.9 for seven modes (seven modes used rather than the more common six to allow direct comparison with seven-core fiber).

FMF presents a problem for integrated MCS technology, because switches and splitters are difficult to implement in PLC waveguides. We assume that free-space switches (MEMS-based) and free-space beamsplitters are used instead to realize the MCS functionality, and that this can be done for roughly the same cost as the integrated version [87]. The sizes of the MEMS mirrors and beamsplitters would need to be increased to accommodate the multimode beams, but otherwise the MCS design would be similar to a single-mode version. We estimate the MCS cost to be increased by a factor of 1.3 for three modes and by a factor of 1.7 for seven modes.

Estimating the amplifier cost for multimode fiber is a challenge because multimode amplifier demonstrations to date fall short of present-day performance requirements, particularly in transient suppression, gain flatness, and power efficiency. We note only that the cost increase must fall between a factor of 1 (same cost as conventional amplifier) and a cost increase of 3 or 7 (which results if we amplify the modes separately with three or seven conventional single-mode amplifiers; if the multimode amplifier cost is higher than this we use instead multiple single-mode amplifiers). So we choose intermediate values and assume a cost increase of 2 times for three modes, and 3.5 times for seven modes.

C. Multi-Core Fiber Systems

For MCF with joint switching, the architecture again looks like that of Fig. 19, but with all components compatible with multi-core fiber. The most practical method of making a WSS compatible with MCF is with spatial diversity, where the multiple cores are separated and jointly switched (possibly with the remapping function to reduce the steering angle requirements). This makes the WSS realizable using today's WSS switching engine technology. The cost increase for seven-core fiber is estimated to be a factor of 3.6, which includes a factor of two because the large port count precludes making a Twin device, and a factor of 1.8 to account for the large port count. Note that the cost for an MCF-compatible WSS is estimated to be higher than the FMF-compatible WSS due to the stringent requirement to maintain core isolation, which leads to larger pitch fiber and collimator arrays and bigger overall implementation.

For an MCS compatible with seven-core fiber, one could break out the modes and use seven conventional integrated MCSs; however, this results in a cost increase of ×7. Instead, we assume that MCS can utilize free-space components designed to accommodate seven modes per mirror and beamsplitter, which results in a cost increase of only about 3.4, taking advantage of the assumption that we need only switching with wavelength granularity, in which case free-space optics can provide better cost scaling than integrated optics because the number of components does not increase with the number of cores. If lane (or core)-change capability is required with MCF, the architecture becomes similar to the overlay configuration, with comparable cost.

For integrated MCF amplifiers, we assume a cost increase between the limits of 1 and 7, where we use a cost increase of 3.5 times for the seven-core fiber amplifier in our cost estimates.

The wavelength-granularity switching strategy (joint switching in the space domain) can be applied to the single-mode fiber overlay architecture, with cost savings achieved by making use of the same WSS and MCS components we proposed for the MCF ROADM architecture with wavelength granularity. The resulting costs are similar to those for the MCF ROADM architecture (which are much lower than the costs for the case of overlay fibers employing ROADM with space–wavelength granularity), except that the amplifier cost would be seven times for a 7× overlay (one amplifier

per MCF common port). Alternatively, switching with fractional space, full wavelength granularity could be implemented, which would have a cost intermediate between those of switching with wavelength granularity and with space–wavelength granularity.

D. Multi-Band Extended Systems

Finally, we consider extending the operating wavelength range to the L and S bands as a means of increasing capacity. The most straightforward approach would be to separate the bands and have duplicate WSSs, MCSs, and amplifiers for each band (presuming S-band amplifiers become available), which increases the capacity by 2 or 3 times but at 2 or 3 times the ROADM cost. Two alternatives may emerge: The first requires a redesign of the WSS to support a larger communication band at the same resolving power as today's systems. This faces design challenges, as the WSS complexity scales with the number of resolvable points (or bandwidth support/optical resolution). As a cost-saving alternative, we propose to preserve WSS complexity (i.e., the resolvable points) and accompany the extended bandwidth with a coarser spectral resolution by inserting a lower dispersion diffraction grating. Hence, this would enable extended band coverage without increasing the WSS cost. This does have the significant disadvantage that the channel width must increase to maintain spectral efficiency, so it is unlikely to be adopted, but for the sake of presenting cost-saving options we consider it here. We assume that the WSS and MCS costs are unchanged (it is assumed that an MCS can be made to cover the extended frequency range), but we consider separate amplifiers for each band, so an amplifier cost scaling of 2 or 3 times for two or three bands. It is worth pointing out that much of the apparent cost savings of this approach is simply due to the increase in size of the switchable data unit (the increased channel width), which results in fewer A/D ports needed for a given volume of dropped traffic. This cost-saving technique is being applied to current networks, through the use of superchannels, with no change to the ROADM infrastructure, provided it is capable of handling flexible channel widths. However, with lesser spectral resolving power, the guard bands between superchannels would have to be increased, thereby negatively impacting spectral utilization, i.e., capacity.

E. Cost Comparison

Combining all of the calculations and cost projections on future devices, we arrive at the chart shown in Fig. 20, comparing the normalized ROADM cost per bit for the various options. The main takeaways from this chart are the rapidly increasing costs for the overlay approach with independent switching, and that capacity expansion options with joint switching (FMF, MCF, and overlays) result in lower costs than the baseline.

We emphasize that this analysis considers only the cost of ROADM components. To make an architecture decision requires consideration of all costs, of which this is only a part. The actual SDM fiber may dominate the cost, and operators may first choose the overlay solutions which utilize an already available SMF plant buried in the ground.

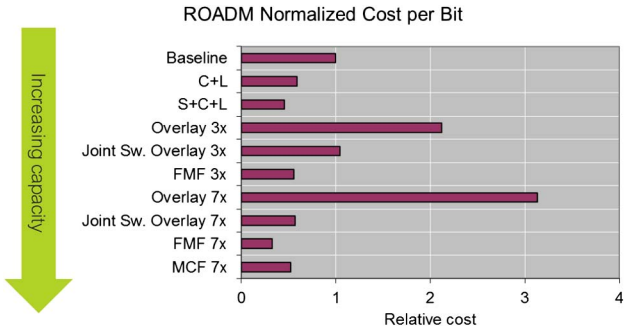

Fig. 20. Comparison of ROADM normalized costs for considered capacity expansion options.

VI. Conclusion and Outlook

The persistent growth of traffic carried by optical networks, coupled with the fact that all the "easy" solutions to exploit the optical bandwidth available across the conventional communication band have been exhausted, implies that new measures will have to be taken in the years ahead to achieve additional network capacity. In this survey paper we have outlined several measures, all introducing innovations in optical switching systems to fully utilize the spectral domain and further extend into the spatial domain. EON will allow for the full exploitation of the C-band, with information-bearing signals having minimal GBs between wide superchannels. Technologies in support of subchannel addition and extraction within the superchannel for signals with fine GBs between them or even spectrally overlapping have been identified. After fully exploiting the conventional communication band, additional information can be encoded beyond its spectrum (extension to the long and short bands) or to the spatial domain (SMF overlays or new SDM fibers). WSS solutions for all these scenarios have been discussed. The spatial domain promises a larger capacity multiplier. However, network realizations with high-channel-count SDM solutions must provide the capacity benefits at small incremental costs (sublinear) for the network to scale in a cost-effective manner in support of the projected capacity increases. We identify that some measure of loss of routing flexibility may need to be incurred, whether in the frequency or space domains or in a combination of both, to obtain significant equipment and cost reduction. The networking impact of such routing restrictions continues to be a topic of debated research.

As the switching solutions introduced in support of SDM–WDM information encoding can adapt to all fiber types (multiple SMF, FMF, MCF), we can safely conclude that the switches alone will not serve as the determining factor in the identification of the optimal SDM solution. Additional factors include optical amplifiers (their cost, gain value and uniformity, and noise figure), receiver complexity (for cases where MIMO

processing is required), the cost of producing the fiber medium itself, and networking efficiency. However, the SDM–WDM ROADM implementation complexity and cost may indeed be influential. Taken together, we can imagine in one extreme case a multimode fiber supporting a large spatial channel count (at least an order of magnitude increase in capacity). In this case, channels are prone to mixing and hence must be jointly switched. The ROADM implementation is the simplest of all SDM–WDM switching solutions, having the same WSS count per node as in SMF networks (but with modified WSSs), and will incorporate integrated SDM transceivers and MIMO processing. If multimode optical fiber amplifiers are used, this solution appears to be the least expensive. However, spatial channel utilization and fragmentation under different network loads will lower the overall efficiency. At the opposite extreme, the cases of MCF with well-isolated cores or parallel SMF links will experience no mixing in transmission. The ROADM node complexity will be compounded when the switching granularity is as fine as the individual wavelength and spatial channel due to many switching modules required for its implementation. However, the system can utilize today's single-channel transceivers. This solution will likely benefit the least from SDM integration, and hence the capacity increase will be accompanied by escalating cost, which may make this solution unattractive. Overall SDM system tradeoffs in switching granularity need to be considered together with networking efficiency, cost, and technology maturation, which will likely take a few more years—until the traffic volumes required for delivery cannot be well-sustained by the existing infrastructure.

The need to extend beyond optical networks operating on the conventional communication band supported by SMF represents a great opportunity for optical technology innovation, ranging from the fiber to ancillary components and subsystems. In this paper, we have highlighted the switching solutions we foresee to address this challenge and discussed the merits and demerits of each proposed ROADM node implementation (see Table II for our comparative summary). However, we anticipate there is room for additional innovation and ingenuity in this space, and encourage additional research in this developing and significant field.

Acknowledgment

This work was supported in part by the European Commission's Seventh Framework Program under Grant Agreements 318415 (FOX-C project) and 619732 (INSPACE project).

References

[1] P. J. Winzer, "Spatial multiplexing in fiber optics: The 10× scaling of metro/core capacities," *Bell Labs Tech. J.*, vol. 19, pp. 22–30, 2014.

[2] "Cisco Visual Networking Index: Forecast and methodology, 2015–2020," June 2016.

[3] A. D. Ellis, J. Zhao, and D. Cotter, "Approaching the nonlinear Shannon limit," *J. Lightwave Technol.*, vol. 28, no. 4, pp. 423–433, 2010.

[4] R. Essiambre, G. Kramer, P. J. Winzer, G. J. Foschini, and B. Goebel, "Capacity limits of optical fiber networks," *J. Lightwave Technol.*, vol. 28, no. 4, pp. 662–701, 2010.

[5] O. Gerstel, M. Jinno, A. Lord, and S. J. B. Yoo, "Elastic optical networking: A new dawn for the optical layer?" *IEEE Commun. Mag.*, vol. 50, no. 2, pp. s12–s20, 2012.

[6] I. Tomkos, S. Azodolmolky, J. Solé-Pareta, D. Careglio, and E. Palkopoulou, "A tutorial on the flexible optical networking paradigm: State-of-the-art, trends, and research challenges," *Proc. IEEE*, vol. 102, no. 9, pp. 1317–1337, 2014.

[7] D. Klonidis, S. Sygletos, D. M. Marom, S. Fabbri, A. Ellis, E. Pincemin, C. Betoule, G. Thouenon, D. Hillerkuss, B. Baeuerle, A. Josten, J. Leuthold, J. Zhao, S. Ben-Ezra, J. F. Ferran, M. Angelou, G. Papastergiou, P. Zakynthinos, and I. Tomkos, "Enabling transparent technologies for the development of highly granular flexible optical cross-connects," in *Proc. 16th Int. Conf. Transparent Optical Networks (ICTON)*, 2014, paper We.D1.5.

[8] B. Shariati, P. S. Khodashenas, J. M. Rivas-Moscoso, S. Ben-Ezra, D. Klonidis, F. Jiménez, L. Velasco, and I. Tomkos, "Investigation of mid-term network migration scenarios comparing multi-band and multi-fiber deployments," presented at the Optical Fiber Communication Conf. and Exhibition (OFC), Anaheim, CA, Mar. 2016, paper Th1E.1.

[9] F. Farjady, N. Antoniades, R. E. Wagner, and M. J. Yadlowsky, "Value of fiber overlays in WDM metro networks," *IEEE Photon. Technol. Lett.*, vol. 15, no. 2, pp. 329–331, 2003.

[10] K. Nakajima, P. Sillard, D. Richardson, M.-J. Li, R.-J. Essiambre, and S. Matsuo, "Transmission media for an SDM-based optical communication system," *IEEE Commun. Mag.*, vol. 53, no. 2, pp. 44–51, 2015.

[11] M. D. Feuer, L. E. Nelson, X. Zhou, S. L. Woodward, R. Isaac, B. Zhu, T. F. Taunay, M. Fishteyn, J. M. Fini, and M. F. Yan, "Joint digital signal processing receivers for spatial superchannels," *IEEE Photon. Technol. Lett.*, vol. 24, no. 21, pp. 1957–1960, 2012.

[12] L. E. Nelson, M. D. Feuer, K. Abedin, X. Zhou, T. F. Taunay, J. M. Fini, B. Zhu, R. Isaac, R. Harel, G. Cohen, and D. M. Marom, "Spatial superchannel routing in a two-span ROADM system for space division multiplexing," *J. Lightwave Technol.*, vol. 32, no. 4, pp. 783–789, 2014.

[13] D. M. Marom, J. Dunayevsky, D. Sinefeld, M. Blau, R. Ryf, N. K. Fontaine, M. Montoliu, S. Randel, C. Liu, B. Ercan, M. Esmaeelpour, S. Chandrasekhar, A. H. Gnauck, S. G. Leon-Saval, J. Bland-Hawthorn, J. R. Salazar-Gil, Y. Sun, L. Grüner-Nielsen, and R. Lingle, Jr., "Wavelength-selective switch with direct few mode fiber integration," *Opt. Express*, vol. 23, no. 5, pp. 5723–5737, 2015.

[14] D. Siracusa, F. Pederzolli, P. Khodashenas, J. M. Rivas-Moscoso, D. Klonidis, E. Salvadori, and I. Tomkos, "Spectral vs. spatial superchannel allocation in SDM networks under independent and joint switching paradigms," in *Proc. European Conf. Optical Communication (ECOC)*, 2015, paper Mo.4.6.2.

[15] P. S. Khodashenas, J. M. Rivas-Moscoso, D. Siracusa, F. Pederzolli, B. Shariati, D. Klonidis, E. Salvadori, and I. Tomkos, "Comparison of spectral and spatial super-channel allocation schemes for SDM networks," *J. Lightwave Technol.*, vol. 34, no. 11, pp. 2710–2716, 2016.

[16] B. Shariati, P. S. Khodashenas, J. M. Rivas-Moscoso, S. Ben-Ezra, D. Klonidis, F. Jiménez, L. Velasco, and I. Tomkos, "Evaluation of the impact of different SDM switching strategies in a network planning scenario," presented at the Optical Fiber Communication Conf. and Exhibition, Anaheim, CA, Mar. 2016, paper Tu2H.4.

[17] D. T. Nelson, C. R. Doerr, D. M. Marom, R. Ryf, and M. P. Earnshaw, "Wavelength selective switching for optical bandwidth management," *Bell Labs Tech. J.*, vol. 11, no. 2, pp. 105–128, 2006.

[18] P. Colbourne and B. Collings, "ROADM switching technologies," in *Optical Fiber Communication Conf. (OFC)*, 2011, paper OTuD1.

[19] D. M. Marom, D. T. Neilson, D. S. Greywall, C. S. Pai, N. R. Basavanhally, V. A. Aksyuk, D. O. López, F. Pardo, M. E. Simon, Y. Low, P. Kolodner, and C. A. Bolle, "Wavelength-selective $1 \times K$ switches using free-space optics and MEMS micromirrors: Theory, design, and implementation," *J. Lightwave Technol.*, vol. 23, no. 4, pp. 1620–1630, 2005.

[20] R. Ryf, Y. Su, L. Moller, S. Chandrasekhar, X. Liu, D. T. Neilson, and C. R. Giles, "Wavelength blocking filter with flexible data rates and channel spacing," *IEEE J. Lightwave Technol.*, vol. 23, no. 1, pp. 54–61, 2005.

[21] T. A. Strasser and J. L. Wagener, "Wavelength-selective switches for ROADM applications," *IEEE J. Sel. Top. Quantum Electron.*, vol. 16, no. 5, pp. 1150–1157, 2010.

[22] G. Baxter, S. Frisken, D. Abakoumov, H. Zhou, I. Clarke, A. Bartos, and S. Poole, "Highly programmable wavelength selective switch based on liquid crystal on silicon switching elements," in *Optical Fiber Communication Conf. (OFC)*, 2006, paper OTuF2.

[23] D. Sinefeld and D. M. Marom, "Insertion loss and crosstalk analysis of a fiber switch based on a pixelized phase modulator," *J. Lightwave Technol.*, vol. 29, pp. 69–77, 2011.

[24] S. J. Frisken, G. W. Baxter, H. Zhao, and D. Abakoumov, "Optical calibration system and method," U.S. patent 7457547 (Nov. 25, 2008).

[25] S. Frisken, G. Baxter, D. Abakoumov, H. Zhou, I. Clarke, and S. Poole, "Flexible and grid-less wavelength selective switch using LCOS technology," in *Optical Fiber Communication Conf. (OFC)*, 2011, paper OTuM3.

[26] J.-K. Rhee, I. Tomkos, and M.-J. Li, "A broadcast-and-select OADM optical network with dedicated optical-channel protection," *J. Lightwave Technol.*, vol. 21, no. 1, pp. 25–31, 2003.

[27] M. Vasilyev, I. Tomkos, M. Mehendale, J.-K. Rhee, A. Kobyakov, M. Ajgaonkar, S. Tsuda, and M. Sharma, "Transparent ultra-long-haul DWDM networks with "broadcast-and-select" OADM/OXC architecture," *J. Lightwave Technol.*, vol. 21, no. 11, pp. 2661–2672, 2003.

[28] D. T. Neilson, H. Tang, D. S. Greywall, N. R. Basavanhally, L. Ko, D. A. Ramsey, J. D. Weld, Y. L. Low, F. Pardo, D. O. Lopez, P. Busch, J. Prybyla, M. Haueis, C. S. Pai, R. Scotti, and R. Ryf, "Channel equalization and blocking filter utilizing microelectromechanical mirrors," *IEEE J. Sel. Top. Quantum Electron.*, vol. 10, no. 3, pp. 563–569, 2004.

[29] B. Collings, "New devices enabling software-defined optical networks," *IEEE Commun. Mag.*, vol. 51, no. 3, pp. 66–71, 2013.

[30] D. M. Marom, D. T. Neilson, J. Leuthold, M. A. Gibbons, and C. R. Giles, "64 channel 4×4 wavelength-selective crossconnect for 40 Gb/s channel rates with 10 Tb/s throughput capacity," in *Proc. European Conf. Optical Communication (ECOC)*, 2003, pp. 816–817.

[31] J. M. Simmons and A. A. M. Saleh, "Wavelength-selective CDC ROADM designs using reduced-sized optical crossconnects," *IEEE Photon. Technol. Lett.*, vol. 27, no. 20, pp. 2174–2177, 2015.

[32] R. Jensen, A. Lord, and N. Parsons, "Colourless, directionless, contentionless ROADM architecture using low-loss optical matrix switches," in *Proc. European Conf. Optical Communication (ECOC)*, 2010, paper Mo.2.D.2.

[33] E. Hugues-Salas, G. Zervas, D. Simeonidou, E. Kosmatos, T. Orphanoudakis, A. Stavdas, M. Bohn, A. Napoli, T. Rahman, F. Cugini, N. Sambo, S. Frigerio, A. D'Errico, A. Pagano, E. Riccardi, V. López, and J. P. Fernández-Palacios Giménez, "Next generation optical nodes: The vision of the European research project IDEALIST," *IEEE Commun. Mag.*, vol. 53, no. 2, pp. 172–181, 2015.

[34] K. Suzuki, Y. Ikuma, E. Hashimoto, K. Yamaguchi, M. Itoh, and T. Takahashi, "Ultra-high port count wavelength selective switch employing waveguide-based I/O frontend," in *Optical Fiber Communication Conf. (OFC)*, Los Angeles, CA, 2015.

[35] M. Iwama, M. Takahashi, M. Kimura, Y. Uchida, J. Hasegawa, R. Kawahara, and N. Kagi, "LCOS-based flexible grid 1×40 wavelength selective switch using planar lightwave circuit as spot size converter," in *Optical Fiber Communication Conf. (OFC)*, Los Angeles, CA, 2015.

[36] M. Iwama, M. Takahashi, Y. Uchida, M. Kimura, R. Kawahara, S.-I. Matsushita, and T. Mukaihara, "Low loss 1×93 wavelength selective switch using PLC-based spot size converter," in *Proc. European Conf. Optical Communication (ECOC)*, Valencia, Spain, 2015, paper Mo.4.2.2.

[37] Y. Ikuma, K. Suzuki, N. Nemoto, E. Hashimoto, O. Moriwaki, and T. Takahashi, "8×24 wavelength selective switch for low-loss transponder aggregator," presented at the Optical Fiber Communication Conf. (OFC), Los Angeles, CA, Mar. 2015, paper Th5A.4.

[38] P. Colbourne, "$M \times N$ wavelength selective optical switch," U.S. patent 20100172646 A1 (July 8, 2010).

[39] Y. Yan, H. Zhao, L. Zong, and Z. Feng, "8×128 adWSS for CDC ROADM," in *Int. Conf. Photonics in Switching (PS)*, Florence, Italy, Sept. 2015, paper WeI2.5.

[40] L. Pascar, R. Karubi, B. Frenkel, and D. M. Marom, "Port-reconfigurable, wavelength-selective switch array for colorless/directionless/contentionless optical add/drop multiplexing," presented at Int. Conf. Photonics in Switching (PS), Florence, Italy, Sept. 2015, paper PDP.2.

[41] R. Ryf, P. Bernasconi, P. Kolodner, J. Kim, J. P. Hickey, D. Carr, F. Pardo, C. Bolle, R. Frahm, N. Basavanhally, C. Yoh, D. Ramsey, R. George, J. Kraus, C. Lichtenwalner, R. Papazian, J. Gates, H. R. Shea, A. Gasparyan, V. Muratov, J. E. Griffith, J. A. Prybyla, S. Goyal, C. D. White, M. T. Lin, R. Ruel, C. Nijander, S. Amey, D. T. Neilson, D. J. Bishop, S. Pau, C. Nuzman, A. Weis, B. Kumar, D. Lieuwen, V. Aksyuk, D. S. Greywall, T. C. Lee, H. T. Soh, W. M. Mansfield, S. Jin, W. Y. Lai, H. A. Huggins, D. L. Barr, R. A. Cirelli, G. R. Bogart, K. Teffeau, R. Vella, H. Mavoori, A. Ramirez, N. A. Ciampa, F. P. Klemens, M. D. Morris, T. Boone, J. Q. Liu, J. M. Rosamilia, and C. R. Giies, "Scalable wavelength-selective crossconnect switch based on MEMS and planar waveguides," in *Proc. European Conf. Optical Communication (ECOC)*, 2001.

[42] N. K. Fontaine, R. Ryf, and D. T. Neilson, "$N \times M$ wavelength selective crossconnect with flexible passbands," in *Optical Fiber Communication Conf. (OFC)*, 2012, paper PDP5B.2.

[43] F. Xiao and K. Alameh, "Opto-VLSI-based $N \times M$ wavelength selective switch," *Opt. Express*, vol. 21, pp. 18160–18169, 2013.

[44] L. Zong, H. Zhao, Z. Feng, and S. Cao, "Demonstration of ultra-compact contentionless-ROADM based on flexible wavelength router," in *Proc. European Conf. Optical Communication (ECOC)*, 2014, paper P.4.4.

[45] L. Zong, H. Zhao, Z. Feng, and Y. Yan, "8 × 8 flexible wavelength cross-connect for CDC ROADM application," *IEEE Photon. Technol. Lett.*, vol. 27, no. 24, pp. 2603–2606, 2015.

[46] N. Nemoto, Y. Ikuma, K. Suzuki, O. Moriwaki, T. Watanabe, M. Itoh, and T. Takahashi, "8 × 8 wavelength cross connect with add/drop ports integrated in spatial and planar optical circuit," in *Proc. European Conf. Optical Communication (ECOC)*, 2015, paper Tu.3.5.1.

[47] L. Zong, H. Zhao, Y. Yan, and Z. Feng, "Demonstration of quasi-contentionless flexible ROADM based on a multiport WXC," *J. Opt. Commun. Netw.*, vol. 8, pp. A141–A151, 2016.

[48] Y. Loussouarn, E. Pincemin, M. Song, S. Gauthier, Y. Chen, and S. Zhong, "400 Gbps real-time coherent Nyquist-WDM DP-16QAM transmission over legacy G.652 or G.655 fibre infrastructure with 2 dB margins," in *Optical Fiber Communication Conf. (OFC)*, Los Angeles, CA, 2015.

[49] S. Melle, A. Deore, O. Turkcu, S. Ahuja, and S. J. Hand, "Comparing optical and OTN switching architectures in next-gen 100 Gb/s networks," presented at the Optical Fiber Communication Conf. and Exhibition, Anaheim, CA, Mar. 2013, paper NM3F-2.

[50] P. S. Khodashenas, J. M. Rivas-Moscoso, D. Klonidis, G. Thouénon, C. Betoule, and I. Tomkos, "Impairment-aware resource allocation over flexi-grid network with all-optical add/drop capability," presented at the European Conf. Optical Communication (ECOC), Valencia, Spain, Sept. 2015, paper P.6.13.

[51] P. S. Khodashenas, J. M. Rivas-Moscoso, D. Klonidis, I. Tomkos, G. Thouénon, C. Betoule, and E. Pincemin, "Techno-economic analysis of flexi-grid networks with all-optical add/drop capability," presented at Int. Conf. Photonics in Switching (PS), Florence, Italy, Sept. 2015, paper ThIII2.2.

[52] G. Thouénon, C. Betoule, E. Pincemin, P. S. Khodashenas, J. M. Rivas-Moscoso, and I. Tomkos, "All-optical vs. electrical aggregations CAPEX comparisons in a fully-flexible multilayer transport network," presented at the European Conf. on Optical Communication (ECOC), Valencia, Spain, Sept. 2015, paper We.4.5.4.

[53] R. Rudnick, A. Tolmachev, D. Sinefeld, O. Golani, S. Ben-Ezra, M. Nazarathy, and D. M. Marom, "Sub-banded/single-subcarrier drop-demux and flexible spectral shaping with a fine resolution photonic processor," in *Proc. European Conf. Optical Communication (ECOC)*, Cannes, France, 2014, paper PD.4.1.

[54] N. Goldshtein, D. Sinefeld, O. Golani, R. Rudnick, L. Pascar, R. Zektzer, and D. M. Marom, "Fine resolution photonic spectral processor using a waveguide grating router with permanent phase trimming," *J. Lightwave Technol.*, vol. 34, no. 23, pp. 379–385, 2016.

[55] "Spectral grids for WDM applications: DWDM frequency grid," ITU-T Recommendation G.694.1, Feb. 2012.

[56] P. S. Khodashenas, J. M. Rivas-Moscoso, B. Shariati, D. M. Marom, D. Klonidis, and I. Tomkos, "Investigation of spectrum granularity for performance optimization of flexible Nyquist-WDM-based optical networks," *J. Lightwave Technol.*, vol. 33, no. 23, pp. 4767–4774, 2015.

[57] P. Torres-Ferrera, J. M. Rivas-Moscoso, D. Klonidis, D. M. Marom, R. Gutiérrez-Castrejón, and I. Tomkos, "Filtering effects of cascaded flexgrid ROADMs with high spectral resolution filters on the transmission of Nyquist and quasi-Nyquist WDM superchannels," in *Proc. 13th Int. Conf. Optical Communication Networks (ICOCN)*, Suzhou, China, 2014, paper M12.6.

[58] M. Song, E. Pincemin, A. Josten, B. Baeuerle, D. Hillerkuss, J. Leuthold, R. Rudnick, D. M. Marom, S. Ben Ezra, J. F. Ferran, G. Thouenon, P. S. Khodashenas, J. M. Rivas-Moscoso, C. Betoule, D. Klonidis, and I. Tomkos, "Flexible optical cross-connects for high bit rate elastic photonic transport networks," *J. Opt. Commun. Netw.*, vol. 8, pp. A126–A140, 2016.

[59] M. Song, E. Pincemin, B. Baeuerle, A. Josten, D. Hillerkuss, J. Leuthold, R. Rudnick, D. M. Marom, S. Ben-Ezra, J. F. Ferran, S. Sygletos, A. Ellis, J. Zhao, G. Thouenon, C. Betoule, J. M. Rivas, D. Klonidis, and I. Tomkos, "Cascaded all-optical subchannel add/drop multiplexing from a 1-Tb/s super-channel having 2-GHz guard-bands," in *Int. Conf. Photonics Switching (PS)*, Niigata, Japan, July 2016.

[60] L. Zhuang, C. Zhu, Y. Xie, M. Burla, C. G. H. Roeloffzen, M. Hoekman, B. Corcoran, and A. J. Lowery, "Nyquist-filtering (de)multiplexer using a ring resonator assisted interferometer circuit," *J. Lightwave Technol.*, vol. 34, no. 8, pp. 1732–1738, 2016.

[61] B. Corcoran, C. Zhu, J. Schröder, L. Zhuang, B. Foo, M. Burla, W. P. Beeker, A. Leinse, C. G. H. Roeloffzen, and A. J. Lowery, "Multipass performance of a chip-enhanced WSS for Nyquist-WDM sub-band switching," *J. Lightwave Technol.*, vol. 34, no. 8, pp. 1824–1830, 2016.

[62] P. J. Winzer, "An opto-electronic interferometer and its use in subcarrier add/drop multiplexing," *J. Lightwave Technol.*, vol. 31, no. 11, pp. 1775–1782, 2013.

[63] T. Richter, C. Schmidt-Langhorst, R. Elschner, T. Kato, T. Tamimura, S. Watanabe, and C. Schubert, "Coherent in-line substitution of OFDM subcarriers using fiber-frequency conversion and free-running lasers," in *Optical Fiber Communication Conf. (OFC)*, San Francisco, CA, 2014.

[64] S. Sygletos, S. J. Fabbri, E. Giacoumidis, M. Sorokina, D. M. Marom, M. F. C. Stephens, D. Klonidis, I. Tomkos, and A. D. Ellis, "A novel architecture for all-optical add-drop multiplexing of OFDM signals," in *Proc. European Conf. Optical Communication (ECOC)*, Cannes, France, 2014, paper We.1.5.4.

[65] D. Hillerkuss, R. Schmogrow, T. Schellinger, M. Jordan, M. Winter, G. Huber, T. Vallaitis, R. Bonk, P. Kleinow, F. Frey, M. Roeger, S. Koenig, A. Ludwig, A. Marculescu, J. Li, M. Hoh, M. Dreschmann, J. Meyer, S. Ben-Ezra, N. Narkiss, B. Nebendahl, F. Parmigiani, P. Petropoulos, B. Resan, A. Oehler, K. Weingarten, T. Ellermeyer, J. Lutz, M. Moeller, M. Huebner, J. Becker, C. Koos, W. Freude, and J. Leuthold, "26 Tbit s-1 line-rate super-channel transmission utilizing all-optical fast Fourier transform processing," *Nat. Photonics*, vol. 5, no. 6, pp. 364–371, 2011.

[66] S. J. Fabbri, S. Sygletos, A. Perentos, E. Pincemin, K. Sugden, and A. D. Ellis, "Experimental implementation of an all-optical interferometric drop, add, and extract multiplexer for superchannels," *J. Lightwave Technol.*, vol. 33, no. 7, pp. 1351–1357, 2015.

[67] D. M. Marom and M. Blau, "Switching solutions for WDM-SDM optical networks," *IEEE Commun. Mag.*, vol. 53, no. 2, pp. 60–68, 2015.

[68] R. Ramamurthy and B. Mukherjee, "Fixed-alternate routing and wavelength conversion in wavelength-routed optical networks," *IEEE/ACM Trans. Netw.*, vol. 10, no. 3, pp. 351–367, 2002.

[69] I. P. Kaminow, C. R. Doerr, C. Dragone, T. Koch, U. Koren, A. A. M. Saleh, A. J. Kirby, C. M. Ozveren, B. Schofield, R. E. Thomas, R. A. Barry, D. M. Castagnozzi, V. W. S. Chan, B. R. Hemenway, D. Marquis, S. A. Parikh, M. L. Stevens, E. A. Swanson, S. G. Finn, and R. G. Gallager, "A wideband all-optical WDM network," *IEEE J. Sel. Areas Commun.*, vol. 14, no. 5, pp. 780–799, 1996.

[70] P. J. Winzer, "Making spatial multiplexing a reality," *Nat. Photonics*, vol. 8, pp. 345–348, 2014.

[71] D. Richardson, J. Fini, and L. Nelson, "Space-division multiplexing in optical fibres," *Nat. Photonics*, vol. 7, pp. 354–362, 2013.

[72] A. Muhammad, G. Zervas, D. Simeonidou, and R. Forchheimer, "Routing, spectrum and core allocation in flexgrid SDM networks with multi-core fibers," in *Int. Conf. Optical Network Design and Modeling (ONDM)*, 2014, pp. 192–197.

[73] R. Proietti, L. Liu, R. P. Scott, B. Guan, C. Qin, T. Su, F. Giannone, and S. J. B. Yoo, "3D elastic optical networking in the temporal, spectral, and spatial domains," *IEEE Commun. Mag.*, vol. 53, no. 2 pp. 79–87, 2015.

[74] D. Siracusa, F. Pederzolli, D. Klonidis, V. Lopez, and E. Salvadori, "Resource allocation policies in SDM optical networks (invited paper)," in *Int. Conf. Optical Network Design and Modeling (ONDM)*, 2015, pp. 168–173.

[75] D. Klonidis, F. Cugini, O. Gerstel, M. Jinno, V. Lopez, E. Palkopoulou, M. Sekiya, D. Siracusa, G. Thouenon, and C. Betoule, "Spectrally and spatially flexible optical network planning and operations," *IEEE Commun. Mag.*, vol. 53, no. 2, pp. 69–78, 2015.

[76] B. Huang, N. K. Fontaine, R. Ryf, B. Guan, S. G. Leon-Saval, R. Shubochkin, Y. Sun, R. Lingle, and G. Li, "All-fiber mode-group-selective photonic lantern using graded-index multimode fibers," *Opt. Express*, vol. 23, no. 1, pp. 224–234, 2015.

[77] N. K. Fontaine, R. Ryf, J. Bland-Hawthorn, and S. G. Leon-Saval, "Geometric requirements for photonic lanterns in space division multiplexing," *Opt. Express*, vol. 20, no. 24, pp. 27123–27132, 2012.

[78] S. G. Leon-Saval, N. K. Fontaine, J. R. Salazar-Gil, B. Ercan, R. Ryf, and J. Bland-Hawthorn, "Mode-selective photonic lanterns for space-division multiplexing," *Opt. Express*, vol. 22, pp. 1036–1044, 2014.

[79] A. M. Velazquez-Benitez, J. E. Antonio-Lopez, J. C. Alvarado-Zacarias, G. Lopez-Galmiche, P. Sillard, D. Van Ras, C. Okonkwo, H. Chen, R. Ryf, N. K. Fontaine, and R. Amezcua-Correa, "Scaling the fabrication of higher order photonic lanterns using microstructured preforms," in *Proc. European Conf. Optical Communication (ECOC)*, 2015, paper Tu.3.3.2.

[80] N. K. Fontaine, R. Ryf, H. Chen, A. V. Benitez, B. Guan, R. Scott, B. Ercan, S. J. B. Yoo, L. E. Grüner-Nielsen, Y. Sun, R. Lingle, E. Antonio-Lopez, and R. Amezcua-Correa, "30 × 30 MIMO transmission over 15 spatial modes," in *Optical Fiber Communication Conf. (OFC)*, 2015, paper Th5C.1.

[81] Y. Ikuma, K. Suzuki, N. Nemoto, E. Hashimoto, O. Moriwaki, and T. Takahashi, "Low-loss transponder aggregator using spatial and planar optical circuit," *J. Lightwave Technol.*, vol. 34, no. 1, pp. 67–72, 2016.

[82] K. Suzuki, M. Nakajima, K. Yamaguchi, G. Takashi, Y. Ikuma, K. Shikama, Y. Ishii, M. Itoh, M. Fukutoku, T. Hashimoto, and Y. Miyamoto, "Wavelength selective switch for multi-core fiber based space division multiplexed network with core-by-core switching capability," in *Int. Conf. Photonics Switching (PS)*, Niigata, Japan, July 2016.

[83] J. Carpenter, S. G. Leon-Saval, J. R. Salazar-Gil, J. Bland-Hawthorn, G. Baxter, L. Stewart, S. Frisken, M. A. F. Roelens, B. J. Eggleton, and J. Schröder, "1 × 11 few-mode fiber wavelength selective switch using photonic lanterns," *Opt. Express*, vol. 22, no. 3, pp. 2216–2221, 2014.

[84] N. K. Fontaine, R. Ryf, C. Liu, B. Ercan, J. R. Salazar Gil, S. G. Leon-Saval, J. Bland-Hawthorn, and D. T. Neilson, "Few-mode fiberwavelength selective switch with spatial-diversity and reduced-steering angle," in *Optical Fiber Communication Conf. (OFC)*, 2014, paper Th4A.7.

[85] N. K. Fontaine, T. Haramaty, R. Ryf, H. Chen, L. Miron, L. Pascar, M. Blau, B. Frenkel, L. Wang, Y. Messaddeq, S. LaRochelle, R. J. Essiambre, Y. Jung, Q. Kang, J. K. Sahu, S. U. Alam, D. J. Richardson, and D. M. Marom, "Heterogeneous space-division multiplexing and joint wavelength switching demonstration," in *Optical Fiber Communication Conf. (OFC)*, 2015, paper Th5C.5.

[86] R. Ryf, N. K. Fontaine, J. Dunayevsky, D. Sinefeld, M. Blau, M. Montoliu, S. Randel, C. Liu, B. Ercan, M. Esmaeelpour, S. Chandrasekhar, A. H. Gnauck, S. G. Leon-Saval, J. Bland-Hawthorn, J. R. Salazar-Gil, Y. Sun, L. Grüner-Nielsen, R. Lingle, Jr., and D. M. Marom, "Wavelength-selective switch for few-mode fiber transmission," in *Proc. European Conf. Optical Communication (ECOC)*, 2013, paper PD1.C.4.

[87] Y. Jung, S. Alam, and D. J. Richardson, "Compact few-mode fiber collimator and associated optical components for mode division multiplexed transmission," in *Optical Fiber Communication Conf. (OFC)*, 2016, paper W2A.40.

Dan M. Marom (S'99-M'00-SM'08) received the B.Sc. degree in mechanical engineering and the M.Sc. degree in electrical engineering, both from Tel-Aviv University, Israel, in 1989 and 1995, respectively, and was awarded a Ph.D. in electrical engineering from the University of California, San Diego (UCSD), in 2000.

From 2000 until 2005, he was a Member of the Technical Staff at the Advanced Photonics Research Department of Bell Laboratories, Lucent Technologies, where he invented and headed the research and development effort of MEMS-based wavelength-selective switching solutions for optical networks. Since 2005, he has been with the Applied Physics Department, The Hebrew University of Jerusalem, Israel, where he is now an Associate Professor leading the Photonics Devices research group and pursuing his research interests in creating photonic devices and sub-systems for switching and manipulating optical signals in guided-wave and free-space optics solutions using light modulating devices, nonlinear optics, and compound materials.

Prof. Marom is a Senior Member of the IEEE Photonics Society and a Fellow of The Optical Society (OSA). He was awarded the IEEE Photonics Society Distinguished Lecturer Award for 2014 and extended to 2015. From 1996 through 2000, he was a Fannie and John Hertz Foundation Graduate Fellow at UCSD, and was a Peter Brojde Scholar in 2006–2007. He currently serves as one of two Senior Editors for *Photonics Technology Letters*, handling all photonic-device-related submissions.

Paul D. Colbourne received the B.Sc. degree in mechanical engineering from Mount Allison University, Sackville, Nova Scotia, Canada in 1983; the B.Eng. degree in engineering physics from the Technical University of Nova Scotia (now Dalhousie University), Halifax, Nova Scotia, Canada in 1986; and the M.Eng. degree and Ph.D. degree in engineering physics from McMaster University, Hamilton, Ontario, Canada in 1988 and 1993, respectively

From 1993 to the present he has been at Lumentum (formerly JDSU), designing components for fiber optic systems, including tunable filters, dispersion compensators, the Swept Wavelength System, wavelength blockers, and, most recently, wavelength-selective switches. He holds more than 40 U.S. patents.

Dr. Colbourne is a member of The Optical Society (OSA) and served on the Technical Committee for OFC 2006–2008.

Antonio D'Errico, received the Ph.D. degree *cum laude* in telecommunication engineering from the Scuola Superiore Sant'Anna, Pisa, Italy, in 2008. Since 2009, he has been with Ericsson Research as a

Senior Researcher in photonics and telecommunication systems. His research interests also include advanced technological solutions for optical networks. He is now working on photonic enabling technologies toward 5G Mobile Networks. He is author of more than 80 papers published in international journals, conference digests, and patents. He is on the board of reviewers for a number of international journals in the fields of optics and photonics.

Nicolas K. Fontaine obtained his Ph.D. degree in electrical engineering at the University of California, Davis, in the Next Generation Network Systems Laboratory [http://sierra.ece.ucdavis.edu] in 2010. In his dissertation, he studied how to generate and measure the amplitude and phase of broadband optical waveforms in many narrowband spectral slices.

Since June 2011, he has been a Member of the Technical Staff at Bell Laboratories in Crawford Hill, New Jersey, in the Advanced Photonics Division. At Bell Labs, he develops devices for space-division multiplexing in multi-core and few-mode fibers, builds wavelength cross-connects and filtering devices, and investigates spectral slice coherent receivers for THz bandwidth waveform measurement. He serves on the OFC Technical Program Committee on fiber devices, the CLEO Technical Program Committee on lightwave communications, is an Associate Editor for *IEEE Photonics Journal*, and is General Co-chair for The Optical Society (OSA) NETWORKS 2016 meeting.

Yuichiro Ikuma (S'07-M'12) was born in Kanagawa, Japan, in 1985. He received B.E., M.E., and Ph.D. degrees in electronics and electrical engineering from Keio University, Yokohama, Japan, in 2007, 2009, and 2012, respectively. From 2009 to 2012, he was a Research Fellow of the Japan Society for the Promotion of Science.

Since he joined NTT Photonics Laboratories in 2012, he has been involved in the development of optical switches for ROADM systems. He is currently with NTT Network Service Systems Laboratories, Musashino, Japan.

Dr. Ikuma is a member of the IEEE Photonics Society and Institute of Electronics, Information and Communication Engineers (IEICE) of Japan.

Roberto Proietti's biography was not available at the time of publication.

Liangjia Zong was born in Jiangxi, China, in 1984. He received the B.Sc. degree in optical information science and technology, and the Ph.D. degree in physical electronics, from Huazhong University of Science and Technology, Wuhan, China, in 2006 and 2011, respectively.

He then joined Huawei as a Research Engineer in the Transmission Technology Research Department. His research includes high-speed optical transmission systems and all-optical switching technology. He has authored over 40 papers published in peer-reviewed journals, international conferences, and patents.

José Manuel Rivas-Moscoso obtained his Ph.D. in physics from the University of Santiago de Compostela, Spain, in 2004. From 2004 to 2010, he worked as a Postdoctoral Researcher at the Cambridge University Engineering Department, Cambridge, UK, and the School of Telecommunication of the Technical University of Madrid, Spain.

In 2011, he joined the Network Core Evolution Group at Telefónica I + D, Spain, where he worked on beyond-100G transport technologies. Since 2014, he has been working with the Network and Optical Communications Group at AIT, Greece. His research interests include elastic optical networks, flexible optical switching, and SDM.

Ioannis Tomkos (B.Sc., M.Sc., Ph.D.) has been a Research Director at the Athens Information Technology Center (AIT) since 2002, wherein he was/is involved in many (over 25) EU-funded research projects with a consortium-wide leading role. He currently serves as a Consultant for executives of ICT companies and telecom regulators, Business Mentor for ICT start-up company founders, and Adjunct Professor at the College of Optical Sciences of the University of Arizona and at the Department of Electrical and Computer Engineering of University of Cyprus Information. In the past, he was an Adjunct Professor at Carnegie-Mellon University, (2002–2010), a Senior Scientist at Corning Inc., (1999–2002), and a Research Associate at the University of Athens, Greece (1995–1999).

Dr. Tomkos is a widely recognized expert in the optical networking and broadband access networks community. Together with his colleagues and students, he has authored over 550 peer-reviewed archival articles (with over 370 indexed in IEEE Xplore), including about 150 journal/magazine/book publications and over 400 conference/workshop proceedings papers. For his research work, he has received over 6000 citations and many distinctions and awards. In 2007, he received the prestigious title of "Distinguished Lecturer" of the IEEE Communications Society, and was elected "Fellow" of the Institute of Engineering and Technology–IET (2010) and The Optical Society (OSA) (2012). He has served as the Chair of the International Optical Networking Technical Committee of the IEEE Communications Society (2007–2008), Chairman of the IFIP working group on "Photonic Networking" (2008–2009), Chairman of the OSA Technical Group on Optical Communications (2009–2010), and Chairman of the IEEE Photonics Society Greek Chapter (2010). He was also involved in several high-level IEEE and OSA committees (most notably the OSA/IEEE Tyndall Award Evaluation/Nomination Committee) and in editorial boards of leading scientific journals (including the *Journal of Lightwave Technology* and the *Journal of Optical Communications and Networking*).

130.43.76.191 {ts '2017-01-07 06:56:59'}